LA-UR -80-1414

TITLE: LIGHT-WATER REACTOR SAFETY ANALYSIS CODES

MASTER

AUTHOR(S): J. F. Jackson, V. H. Ransom, L. J. Ybarrondo, and D. R. Liles

SUBMITTED TO: To be presented at the Nuclear Reactor Safety Heat Transfer 1980 Summer School and International Seminar August 25 - September 5, 1980, Dubrovnik, Yugoslavia. To be published in the Proceedings of the International Centre for Heat and Mass Transfer.

University of California

LOS ALAMOS SCIENTIFIC LABORATORY
Post Office Box 1663 Los Alamos, New Mexico 87545
An Affirmative Action/Equal Opportunity Employer

Form No. 836 R3
St. No. 2629
12/78

UNITED STATES
DEPARTMENT OF ENERGY
CONTRACT W-7405-ENG. 36

LIGHT-WATER REACTOR SAFETY ANALYSIS CODES*

J. F. Jackson,[+] V. H. Ransom,[++] L. J. Ybarrondo,[++] and D. R. Liles[+]

[+]Los Alamos Scientific Laboratory
University of California
Los Alamos, New Mexico 87545

[++]Idaho National Engineering Laboratory
EG&G Idaho, Incorporated
Idaho Falls, Idaho 85415

ABSTRACT

A brief review of the evolution of light-water reactor safety analysis codes is presented. Included is a summary comparison of the technical capabilities of major system codes. Three recent codes are described in more detail to serve as examples of currently used techniques. Example comparisons between calculated results using these codes and experimental data are given. Finally, a brief evaluation of current code capability and future development trends is presented.

1. INTRODUCTION

This paper discusses the evolution of light-water reactor (LWR) accident analysis techniques and describes three available computer codes to illustrate current capability. Emphasis is given to the Loss-of-Coolant Accident (LOCA), although the analysis methods discussed can also be used for other postulated accidents. To further limit the scope, the discussion will be restricted to systems-analysis codes, i.e., those that describe the overall thermal-hydraulic behavior of the entire primary, and in some cases, secondary system during an accident.

Most of the analytical development effort over the past 14 years has been devoted to the large-break LOCA. The accident at Three-Mile Island, however, has resulted in an increased priority on techniques that can deal with the much longer transients that ensue from smaller leaks. Although most of the material in this paper will concentrate on the traditional large-break LOCA analysis methods, their applicability to small break accidents will also be discussed where appropriate.

Much of the earlier work also focused on development of licensing, or "evaluation model" (EM) codes. These codes embody a number of agreed upon "conservatisms" in the modeling to conform to established licensing rules. Recently, there has been more emphasis on developing "best-estimate" codes that try to model the system behavior as accurately as possible. Such codes are much more amenable to experimental assessment and can serve to evaluate the safety margins inherent in EM models. Emphasis in this paper is on best-estimate codes.

*Work performed under the auspices of the U.S. Nuclear Regulatory Commission.

In the first section, we trace the development of LWR accident codes from 1966 through the present time. This will include a discussion of the role of analysis in LWR nuclear safety research, followed by a review of some of the important physical phenomena that have been identified, and the associated technical issues that have required resolution. Finally to illustrate the breadth of the effort and the substantial progress that has been achieved, a chart summarizing the historical evolution of safety code capabilities is presented.

The next three sections are devoted to brief descriptions of three recent accident-analysis system codes developed or under development in the United States. This will include selected separate effects and integral systems test data comparisons. The last section briefly summarizes current capabilities and anticipated development activities.

The three system code descriptions given in this chapter include brief discussions of the numerical methods involved. More detailed information on the numerical methods is presented in Appendix A at the end of Chapter 19, where some of the pertinent basic numerical concepts are reviewed and several buzz terms used in the code descriptions are defined. The appendix at the end of this chapter and Appendix B after Chapter 19 present examples of the finite difference equations and solution strategies used in current reactor safety codes.

1.1 The Role of Analysis in LWR Safety

Analysis has played a unique role in nuclear reactor safety for two main reasons. First, the full-scale demonstration experiments (or actual events) that are normally available to evaluate the accident behavior of industrial products (e.g., automobiles and aircraft) are not available nor practical to obtain in the case of nuclear power plants. This is because the diversity of reactor system designs and the numerous potential events to be considered make the required large number of full-scale experiments prohibitively expensive. Consequently, a greater than usual responsibility has been placed on the reactor safety analyst to be rigorous and accurate in the developing and testing of analysis tools.

A second, and perhaps related, reason stems from the philosophy that has evolved in the United States of making extensive use of analysis as an investigative, design, and evaluation tool. Let us briefly examine this philosophy. First, nuclear plants are designed to be clearly safe in normal operation and incorporate substantial allowance for off-normal operation and system/component failures. Second, analyses are used to determine those system/component failures that could affect safety so that appropriate preventative actions may be taken. Third, it is still presumed that some of the system/component failures will occur and that the provided safety features (with margin and redundancy) will keep the nuclear plant safe in spite of such failures. Finally, some of the safety features themselves are assumed to fail during the accidents they are designed to mitigate so the consequences can be analyzed. This process of repeated investigative analysis is used to identify possible weaknesses of nuclear safety systems so they can be rectified. The result is to reduce the credibility of severe nuclear accidents to an acceptably low level. Thus, nuclear-system safety analysis has been and will continue to be a very important element of LWR nuclear safety.

1.2 Scope of Analysis Development

The development of analytical methods for reactor safety analysis has been one of the most comprehensive analytical efforts undertaken in the United States. This effort has involved several national laboratories, industrial firms, government agencies, and many universities working cooperatively. The completeness and accuracy with which LWR transient behavior under LOCA conditions can be modeled has improved steadily. The analytical tools are continuing to be improved and tested to achieve even greater accuracy, predictive reliability, and economy.

The development of these methods has been and continues to be a very challenging task. The physical phenomena that can exist under postulated accident conditions have required the development of new analytical models and associated numerical solution methods. The large number of components and the complexity of accident phenomena have necessitated innovative application of even the most sophisticated modern computers to achieve the desired results in practical computation times.

The requirement to model two-phase flow conditions has either directly or indirectly accounted for the greatest part of the technical development effort. Under LOCA conditions, nonhomogeneous (relative motion between the phases), nonequilibrium (temperature difference between the phases), and in some cases, multidimensional flow effects can be important. New hydrodynamic models had to be developed to account for these phenomena. The presence of two-phase flow also influences the performance of pumps; the flow-through valves, orifices, and postulated breaks; and convective heat transfer mechanisms. The ability to model with accuracy the discharge rate from an assumed system leak is particularly important since it determines the rate of coolant loss and system depressurization.

Another important area is that of heat transfer. Under design conditions, the heat transfer process in a reactor core is in the well characterized subcooled and nucleate boiling regimes. However under postulated accident conditions, the heat transfer extends into the transition and film boiling regimes. During the emergency coolant reflood phase, the maximum core temperature is dependent upon the details of the film boiling process and in particular, on the transition back to nucleate boiling associated with quenching the hot fuel rods. Axial heat conduction along the very steep temperature gradients near the quench front is also very important.

Substantial progress has been made in understanding basic two-phase thermal-hydraulic phenomena and in their quantification with empirical correlations. These phenomena and their characterization have been the topics of several other chapters. The main purpose of systems-analysis computer codes is to synthesize this knowledge into a consistent framework of conservation relations so that they can be applied to practical reactor safety problems. The advantage of computer modeling is that it allows one to treat the complexity inherent in reactor accident behavior. Advances in computer analysis techniques have had to go hand-in-hand with advances in phenomenological modeling. More efficient and reliable numerical solution strategies have had to be developed. Issues such as convergence, accuracy, stability, and economy have also had to be addressed.

For example, one issue of wide discussion has been the formulation of a macroscopic model for two-phase flow.[1] Attempts to formulate the macroscopic Eulerian-type equations for a nonhomogeneous two-phase mixture have

resulted in systems of differential equations that have complex characteristics (sometimes referred to as being ill-posed).[2-4] This may imply an unstable character for solutions to initial-boundary value problems. Several sets of equations have been proposed, even some that have real roots, but there is no single set that has universal acceptance. Most agree that the difficulty is a result of the inability to describe accurately the differential character of all the fluid interactions[5] and the inability to characterize the covariant terms that arise in the integral averaging process. Even though this issue lacks complete resolution, it has not prevented the development of successful numerical models for the flow of two-phase fluids.[6-8] The reason for this is that the imperfection in the differential models primarily affects the short-wave length behavior of the solutions. Generally, these effects are at shorter wave lengths than can be resolved numerically for practical mesh spacings. Thus, the ill-posed issue is of more academic than practical importance as far as the accurate simulation of LWR systems is concerned.

Stable solution behavior is achieved through the damping or numerical dissipation inherent in the schemes used to solve the differential equations. This numerical dissipation is the result of implicitness, use of donored-flux terms, and inherent viscosity associated with the difference operations. The net result is that the shortest wave-length components of the initial data decay and a well-posed numerical initial-boundary-value problem is obtained. The complexity of most models makes analytical investigation of stability impractical. Stability has been achieved by use of methods proven to be stable for simpler problems and then investigated by numerical experimentation with representative test problems.

The accuracy of analytical models and associated numerical schemes has many facets, i.e., accuracy of the physical description, fluid properties, empirical correlations, and numerical discretization. When calculated results are compared to data, all of these inaccuracies are combined. Careful study is required to separate the sources of inaccuracy. Experience with a particular method gained through application to many separate effects and integral system experiments is probably the best and usual assessment technique. The quest for accuracy is sometimes at odds with the need for economy in terms of required computer time. The use of multidimensional and complex system representations can result in very large systems of equations that must be solved with attendant large computational times. The balance between detail of representation and economy is one that can vary, depending upon the end use of the results. If system component interaction is of interest, then the entire system must be represented even if a compromise in detail is required. If, on the other hand, the phenomena of interest are local or of short duration, then a more detailed representation can be used.

A related issue is the trade-off between simple, and often highly empirical, models and more complex models that are rooted more strongly in fundamental principles. Although the more empirical models are often more economical, they may not extrapolate to new (and untested) regimes as reliably as the more fundamental models.

The extensive range of operation of LWR system components under postulated LOCA conditions places an additional burden on the modeler. Small perturbation theory of linear models is too restrictive to be of use under such conditions since many components and the physical phenomena exhibit highly nonlinear behavior over the range of interest. Thus, each system component model needs to be very general and capable of operation over a wide range. As an example, a pump model must be capable of representing the

performance for both positive and negative flow, positive and negative head, forward and reverse rotation, and fluid conditions ranging from subcooled liquid to all vapor. Such comprehensive representation is frequently made difficult by a lack of data covering the range of potential operation.

2. EVOLUTION OF ANALYTICAL METHODS

In the past 14 years, significant progress has been made in all areas of nuclear safety research and development. In particular, the LWR system codes used for safety analysis have improved substantially. The purpose of this section is to summarize the evolution of this improvement.

2.1 Historical Perspective

The year 1966 is a reasonable point of reference from which to measure progress because on October 27, 1966, Mr. H. L. Price, Director of Regulation, U.S. Atomic Energy Commission (AEC) appointed a task force to conduct a review of power reactor emergency core-cooling systems and core protection.[9] Mr. Price's letter of appointment stated, "Because of the increasing size and complexity of nuclear power plants, the AEC regulatory staff and Advisory Committee on Reactor Safeguards (ACRS) have become increasingly interested in the adequacy of emergency core cooling systems and the phenomena associated with core meltdown . . ."

There are four principal driving forces that have contributed to the continual evolution and improvement of nuclear safety system codes in the United States:

1. The appointment and subsequent report of the task force mentioned above,[9]
2. The emergency core-cooling (ECC) hearings,[10]
3. The research and development conducted in accordance with the Water Reactor Safety Program Plans,[4] and
4. The philosophy of nuclear safety design and evaluation that has evolved in the United States.

The codes used by the pressurized-water reactor (PWR) and boiling-water reactor (BWR) vendors have evolved somewhat separately because of the different geometry and transient behavior of the two reactor systems. In fact, the BWR codes used for LOCA analysis have remained relatively constant in form and content although they have been influenced by the substantial changes in the PWR system-analysis codes. The main emphasis in the following discussions will be devoted to the PWR system-analysis code evolution unless otherwise indicated.

FLASH[12] is the genesis of the reactor system codes used for large-break PWR LOCA analysis. It was developed in the U.S. Naval program. The following statements from page vi of Ref. 12 will help illustrate the state of this type of analysis in 1966 and the progress achieved in 14 years.

> "In previous treatments of the loss-of-coolant accident, the primary system has been represented by a single volume filled with steam and water. In some analyses, the steam and water phases have been assumed to be completely separated and in others, to be completely homogeneous. Core cooling has been assumed to be essentially perfect

until the water inventory fell below some preassigned critical value, after which core cooling has been assumed to be essentially zero. In using these treatments, results were found to depend critically upon the a-priori assumptions concerning the separated or homogeneous state of the coolant and on the value assumed for the critical water inventory. In general, it has been impossible to justify any particular set of assumptions on technical grounds."

The authors go on to say,

"It was to avoid the necessity for making these a-priori assumptions that FLASH was developed. FLASH divides the primary system into three volumes, each of which contains both a homogeneous mixture and a separated steam phase. The degree of separation is calculated continuously. The explicit core-cooling calculations avoid the need for any assumptions concerning water inventories."

The authors were also quite realistic about their achievement and were prophetic about where improvements could be made.

"The model used in FLASH represents a considerable simplification of the actual system geometry. On the other hand, the FLASH model attempts to account for the behavior of every component of the primary system during a loss-of-coolant accident. At present, data on the performance of many of these components under the extreme off-design conditions which prevail during a loss-of-coolant accident are unavailable. As this information becomes available, it can be factored in the existing structure of FLASH. For the present, however, FLASH provides a considerable extension of our ability to calculate what might happen in the primary system during a loss-of-coolant accident."

Table I illustrates the chronological development of the principal PWR oriented codes from FLASH and FLASH-2.[13] The RELAP(SE) series[7,14-19] and TRAC[8] have all been sponsored by the U.S. Nuclear Regulatory Commission (USNRC) or its predecessor the Atomic Energy Commission. All the PWR vendor codes have developed in a manner similar in substance to the USNRC-sponsored codes; therefore, they will not be separately addressed for purposes of brevity.

It is important to note that RELAP5/MOD0[12] and TRAC P1A[13] are offset in Table I to illustrate that they represent a quantum step forward in technical capability, flexibility of use, user convenience, level of experimental assessment, and potential economy of operation. RELP5/MOD0 and TRAC P1A were developed because it was clear that the RELAP series up to RELAP4 could not achieve the technical capability, flexibility of use, user convenience, and economy of operation required for best-estimate nuclear safety calculations.

2.2 Technical Evolution of System Codes

Table II illustrates the technical evolution of the computer codes listed in their chronological order of development in Table I. Most of the categories used to classify the capabilities of the codes were previously used in Refs. 20 and 21. These categories are intended to be representative of the significant progress achieved by each code and are not intended to be complete in the absolute sense of listing every improvement each code represented. The most significant advance(s) offered by each code is highlighted by the accented rectangle(s). It is clear that TRAC and RELAP5 are quite superior technically and mechanistically to the other codes.

TABLE I

CHRONOLOGICAL EVOLUTION OF LWR LARGE-BREAK-LOCA SYSTEM CODES

Computer Code Name	Date
A. Homogeneous and Equilibrium Hydrodynamics Equation Base:	
1. FLASH	May 1966
2. RELAPSE	September 1966
3. FLASH-2	April 1967
4. RELAP 2	March 1968
5. RELAP 3	June 1970
6. RELAP4/MOD3	October 1975
7. RELAP4/MOD5	September 1976
8. RELAP4/MOD6	January 1978
9. RELAP4/MOD7	March 1980
B. Nonhomogeneous and Nonequilibrium Hydrodynamics Equation Base	
1. TRAC (P1A and BDO)	P1A - March 1979 BDO - February 1980
2. RELAP 5	May 1979

It is worthwhile reflecting on the continuing incessant drive for technical excellence, completeness, and precision illustrated by Table II. In the ongoing development of LWR technology, plant designs have become more sophisticated, power densities have become higher to improve economy, and available reactor plant sites have become less favorable. At the same time, people have become more concerned about the quality of their environment. These factors, in addition to the four mentioned earlier, generated increasing needs for improved plant integrity, reliability, and assurance of safety system performance. These increasing needs placed further demands and responsibilities on analysts for measureability in design and safety assessment techniques and rigor in their application. The basic principles are recognized. Special emphasis was given to determining the important LOCA physical phenomena, translating the LOCA phenomena into equations, solving the equations numerically, molding the equations in computations, evaluating the relative conservatism and realism of various assumptions, and testing the resultant system computer codes for completeness and precision using data from component and systems experiments.

TABLE 2

TECHNICAL COMPARISON OF LWR LARGE LOCA SYSTEM CODES

CODE CAPABILITIES	FLASH	RELAPSE	FLASH-2	RELAP2	FLASH-4	RELAP3	RELAP4/MOD3	RELAP4/MOD5	RELAP4/MOD7	RELAP4/MOD7	TRAC(P1A/BDO	RELAP5
A. Reactor System Representation												
• PWR	Yes	Yes	Yes	Yes	Yes	Yes	Yes	Yes	Yes	Yes	Yes	Yes
• BWR	No	No	No	Yes	No	Yes	Yes	Yes	Yes	Yes	Yes	No
• Control Volumes	3	3	20	3	20	20	100	75	75	Dyn.Sto. Comp.Sto.Ltd.	Dyn.Sto. Comp.Sto.Ltd.	Dyn. Sto. Comp.Sto.Ltd
• One-Multi-dimensional	Quasi 2 Dim.	Quasi 1 Dim.	Quasi 1 Dim.	Quasi 1 Dim.	Quasi 1 Dim.	Quasi 1 Dim.	1 Dim.	1 Dim.	1 Dim.	1 Dim.	Multi. Dim.	1 Dim.
• ECC system - LPI	Fill Table	Fill Table	Fill Table	Fill Table	Fill Table	Press. Dep.Fill	Press. Dep. Fill	Time/Press. Dep. Fill	Time/Press. Dep. Fill	Time/Press. Dep. Fill	Time/Press. Dep. Fill	Fill Table
- HPI	Hot Vol Only	Fill Table	Fill Table	Fill Table	Fill Table	Press. Dep.Fill	Press. Dep. Fill	Time/Press Dep. Fill	Time/Press. Dep. Fill	Time/Press. Dep. Fill	Time/Press. Dep. Fill	Fill Table
-Accumulator	No	Fill Table	Fill Table	Fill Table	Fill Table	Press. Dep.Fill	N_2 Driven	Control Vol. w/Air	Control Vol. w/Polytropic Air	Control Vol. w/Polytropic Air	Active Control Vol. w/Air	Active Control Vol.w/Air
• Secondary System	Const. h	Flow Dep. Const. h	Improved Linear Models	Flow Dep. Const. h	Improved Linear Models	Flow Dep. Const. h	Yes.w/Min. Control Logic	Yes.w/Min. Control Logic	Yes.Added Natural Conv. HT to MOD5	Yes.Added Natural Conv. HT to MOD5	Adequate Pri./ Sec.Model-Steam Gen. Only	Same as TRAC(P1A/ BDO)
• Trip Logic	No	No	No	No	No	Yes	Yes	Yes	And/or Logic Logic Added	And/or Logic Logic Added	Complex Trip Logic Allowed	Complex Trip LogicAllowed
• Check Valves	No	No	No	No	No	Yes	Yes	Yes	Yes	Yes	Yes	Yes
• Motor Actuated	No	No	No	No	No	No	Yes	Yes	Yes	Yes	Tabular	Yes
B. Hydro Model												
• Homogeneous & Equil.	Yes	Yes	Yes	Yes	Yes	Yes	Yes	Slip Added	Slip Added	Slip Added	No	Inc. as Option
• Momentum Flux	No	No	No	No	No	No	Yes	Yes	Yes	Yes	Yes	Yes
• Nonhomo. & Nonequil.	No	No	No	No	No	No	No	No	No	Explicit Non-equil.ECC Mix	Two Fluid, Six Equations	2 Fluid,Five Equations
• Numerics	Explicit	Explicit	Explicit	Explicit	Implicit	Explicit	Implicit	Implicit	Implicit	Implicit	Semi-orfully-Implicit	Semi-Implicit
• Arbitrar, Network	No	No	Yes	No	Yes	Yes	Yes	Yes	Yes	Yes	Yes	Yes

TABLE 2

TECHNICAL COMPARISON OF LWR LARGE LOCA SYSTEM CODES

CODE CAPABILITIES	FLASH	RELAPSE	FLASH-2	RELAP2	FLASH-4	RELAP3	RELAP4/MOD3	RELAP4/MOD5	RELAP4/MOD6	RELAP4/MOD7	TRAC(P1A/BD0)	RELAP5
C. Model Improvements												
• Fuel												
- Type	Plate	Plate	Plate	Plate	Plate	Pin/ Plate	Pin/Plate	Pin/Plate	Pin/Plate	Pin/Plate	Pin	Pin/Plate
- Average/Hot Channel	Yes Very Simple	Yes Very Simple	Yes Very Simple	Yes Very Simple	Yes Very Simple	Yes	Yes	Yes	Yes	Yes	Yes, 3D Multi-Rod	Yes, Multi-Rod
- Gap	No	No	No	No	No	No	Yes	Yes Ross & Stoute Used	Yes	Yes Advanced Base on FRAP	Yes	No
- Thermal Properties	No	No	No	No	No	Yes	Yes	Yes	Yes	Yes, From MATPRO	Yes	No
- Conduction	No	No	No	No	No	Yes	Yes	Yes	Yes	Yes	Yes	Yes
• Metal-Water Reaction	No	No	Yes	No	Yes	No	Yes	Yes	Yes, Added Cathcart-Paul	Yes	Yes	No
• Reactor Kinetics	Very Limited	Point Kinetics	Improved FLASH	Point Kinetics	Very Limited	Point Kinetics	Point Kinetics	Point Kinetics	Point Kinetics	Point Kinetics	Point Kinetics	Point Kinetics
• Phase Separation	Constant Vel. Steam	Constant Vel. Steam	Constant Vel. Steam	Variable Bubble Rise	Constant Vel. Steam	Constant Vel. Steam	Variable Bubble Rise	Variable Bubble Rise	Variable Bubble Rise	Variable Bubble Rise	Uses Two-Fluid Model	Uses Two-Fluid Model
• Integral Blowdown Reflood Calculation	No	No	No	No	No	No	No	Reflood Model Must Renod. by Hand	Improved Reflood Must Renod by Hand	Automatic Renod.	Automatic Renod.	Yes but not fully Developed
• Metal Heat Conduction	No	No	Yes Lumped	No	Yes Lumped	No	Yes Distributed	Yes Distributed	Yes Distributed	Yes Distributed	Yes Lumped Dist. Pipes	Yes Distributed
• Water/Steam Properties	Limited Iter. Table Lookup	Limited Iter. Table Lookup	Limited Iter. Table Lookup	Limited Iter. Table Lookup w/Mem.	Limited Iter. Table Lookup Sat.Line	Limited Iter. Table Lookup w/Mem.	Extensive Iter. Table Lookup w/Memory	Extensive Iter. Table Lookup w/Memory	Extensive Iter. Table Lookup w/Memory	Extensive Iter. Table Lookup w/Memory	Correlations	Extensive Direct Table Lookup w/Memory
• Heat Transfer Correlations	Conv. Nucleate & Film Boiling Only. Surface Temp. Dictated Transition Between Correlations					7 Modified Transition on Quality, Press., Mass Flux	Improved	Continued Improvement	Improved Correl. & Logic-Diff. Correl. for Blowdown/ Reflood	Improved Correl. & Logic-Dif.. Correl. for Blowdown/ Reflood	1 Set for Entire Trans. Phases Treated Separately	Same as RELAP4/MOD6 Blowdown Faster Logic

TABLE 2

TECHNICAL COMPARISON OF LWR LARGE LOCA SYSTEM CODES

CODE CAPABILITIES	FLASH	RELAPSE	FLASH-2	RELAP2	FLASH-4	RELAP3	RELAP4/MOD3	RELAP4/MOD5	RELAP4/MOD6	RELAP4/MOD7	TRAC(P1A/BDO)	RELAP5
C. Model Improvements (Continued)												
• For/Rev. Loss Coeff.	No	No	No	No	No	No	Yes	Yes	Yes	Yes	No	Yes
• Pump Representation	Time Tables	Time Tables	Time Tables	Time Tables	Time Tables	Time Tables	Homologous Pump Curves	Homologous Pump Curves	Homologous Pump Curves	Homologous Pump Curves	Homologous Pump Curves	Homologous Pump Curves
• Choked Flow Model	Yes	Yes	Yes	Yes	Yes	Yes	Several Options	Several Options	Several Options	Several Options	M Choking Fine Mesh	2 Fluid Bound. Cond.
D. User Convenience												
• Plots	No	No	No	Yes	Yes	Yes	Yes	Yes	Yes	Yes	Yes	Yes
• Restart	No	No	No	No	No	Yes	Yes	Yes	Yes	Yes+Renod.	Yes+Renod. on Restart	Yes
• Automatic Steady-State	No	No	No	No	No	No	No	No	No	Yes,PWR Only	Yes	No
• Input - Free Format	No	No	Yes	No	No	No	Yes	Yes	Yes	Yes	No	Yes
- Input Diagnostics	Limited	Limited	Limited	Limited	Limited	Limited	Processes Beyond 1st Error	Same as RELAP4/MOD3	Same as RELAP4/MOD3	Same as RELAP4/MOD3	Limited	Excellent process all input
E. Computers Used	CDC 6600	IBM 7044	CDC 6600	IBM 7044 CDC 6600 Univac	CDC 6600	IBM 7044 CDC 6600 CDC 7600	IBM360 CDC6600 CDC7600	IBM360 CDC7600	IBM360 CDC7600	CDC7600	CDC7600	CDC7600

3. RELAP4/MOD6 DESCRIPTION AND EXAMPLE COMPUTATIONS

The RELAP4[17-19] computer code was developed to describe the thermal-hydraulic behavior of LWRs subjected to postulated transients such as a loss-of-coolant, pump failure, or nuclear power excursion. It can also analyze the behavior of part of a system, provided the appropriate thermal-hydraulic boundary conditions are supplied. It calculates the interrelated effects of coolant thermal-hydraulics, system heat transfer, and core neutronics. Because the program was developed to solve a large variety of problems, the user must specify the applicable program options and the system to be analyzed.

3.1 Program Status

RELAP4/MOD7[19] is the most recent version of the RELAP4 code to be released for general use. At this time, RELAP4/MOD6[18] is probably the most extensively used version of the code and most of the discussion herein refers to this version. Where appropriate, improvements that are available in MOD7 will be described.

RELAP4/MOD7 is the culmination of an extensive development effort. This series of codes is based on a homogeneous equilibrium fluid model (HEM) to which many refinements have been added to give a partial account for nonhomogeneous and nonequilibrium effects. The advanced codes, TRAC and RELAP5, are based on more fundamental approaches for modeling nonhomogeneous and nonequilibrium two-phase fluid flow, and in this respect, they represent significant departures from the RELAP4 efforts.

In spite of the limitation of the HEM assumption, these codes have served a very useful function and have provided the nuclear industry with a powerful analytical capability. This capability has been utilized extensively in the design of safety systems and has played a key role in the power reactor licensing process. In fact, the RELAP4 code is still the basic analysis tool for demonstrating that the licensing requirements can be met by a particular plant design. The shift of this function to the advanced codes will occur as experience with, and confidence in, these codes is established.

Those versions of RELAP4 up to and including RELAP4/MOD5[17] were intended primarily as blowdown and refill codes, i. e., they were designed to calculate system phenomena from initial operating conditions to the time of pipe rupture, through system decompression, and up to the initiation of core recovery with emergency core coolant. In the RELAP4/MOD6[18] version, the calculational capabilities were extended from blowdown and refill through core reflood for PWR systems. Finally, RELAP4/MOD7[19] includes improved user conveniences and modeling improvements that permit a continuous or integral calculation of the blowdown and reflood phases of a LOCA.

The evolution of RELAP4 has passed through many cycles of model revision and addition to extend its applicability to situations where the basic assumptions were inadequate. This process led to the production of models to account for nonhomogeneous and nonequilibrium effects. These models are not completely general and, consequently, require considerable knowledge on the part of the user to produce correct results. For these reasons, and in view of the progress of the advanced codes, the RELAP4/MOD7 version of the code is to be the last of this series.

3.2 Model Description

The RELAP4/MOD6 program consists of program controls, fluid dynamics models, heat transfer models, and a reactor kinetics model, all coupled by a numerical solution scheme that advances in time. Each of these parts is summarized in the following pragraphs.

Program Controls. The program input features are used to specify the problem dimensions and constants, time-step size, trip controls for reactor-system transient behavior, and output. Controls are also provided for restarting a problem and producing a plotting tape. There are three basic options that are selected by input--Standard RELAP4, RELAP4-EM, and RELAP CONTAINMENT.

Hydrodynamic Model. The basic modeling philosophy embodied in the RELAP4 code is one in which the system to be modeled is divided into a number of subcontrol volumes that are connected by junctions or flow paths. Mass and energy are conserved in each control volume and an approximate momentum equation is used to calculate the flow at each junction. As RELAP4 has evolved, numerous specialized models have been developed to account for phenomena such as phase separation, thermal nonequilibrium, heat-transfer effects, pumps, valves, multiple stream mixing, etc. The user must specify through the program controls which of these models is to be used in a particular problem. Such modeling decisions do influence the results, and care must be taken that the models are not misapplied. The model variations are too numerous to describe in this limited discussion, so the interested reader is referred to the users manuals.[17-19]

The RELAP4 hydrodynamic model is based on the assumption that the flow process is essentially one-dimensional so that area-averaged properties can be represented as functions of one space variable and time. In addition, the basic model assumes a homogeneous and equilibrium mixture exists at each point in the system. The mass, energy, and flow equations are integrated over a fixed control volume to obtain integrated stream-tube differential relations.

The HEM model includes only the mixture mass conservation equation. The basic mass-dependent variable is the fluid total mass or the density in each control volume. The mass fluxes at each junction connected to a control volume are defined by means of a donor formulation, i.e., the fluid properties of the source are used to compute the mass flux. A Wilson bubble rise model[22] can be selected by the user to approximate nonhomogeneous effects in vertical control volumes, and a slip model is available for approximation of nonhomogenous effects in horizontal control volumes. Both of these models use emperical constants specified by the users.

Like the mass equation, the HEM model only includes the mixture total energy equation. The mixture internal energy in the fluid control volume is the fundamental dependent variable and is expressed in terms of the junction energy flux and fluid total enthalpy. Here again, a donor formulation is used to establish the junction energy properties, although an "enthalpy transport" model can be specified to give a partial account for nonhomogenous and non-equilibrium effects. The enthalpy transport model consists of a quasi-steady approximation to the distribution/energy source terms so that the junction or "edge" energies differ from the volume average values in a manner dependent upon the process. This model can be used to approximate the nonequilibrium effects downstream of emergency core coolant (ECC) injection points and to approximate the energy gradients present in the reflood process.

Four basic forms of the fluid flow equation have evolved and are included in RELAP4.[17] Each form is based on a particular set of assumptions. The user must choose the form most appropriate for a particular junction. The four basic forms are: Form 1--Compressible Single-Stream Flow with Momentum Flux, Form 2--Compressible Two-Stream Flow with One-Dimensional Momentum Mixing, Form 3--Incompressible Single-Stream Flow without Momentum Flux, and Form 4--Compressible Single-Stream Integral Momentum Equation.

The choice of the flow equation form depends upon the purpose and detail of the desired calculation. Forms 1 and 2 include a one-dimensional momentum flux term. These are applicable when the control volumes represent a one-dimensional stream tube. Form 2 should be used only when two streams can combine and exchange momenta on a one-dimensional basis. Form 3 provides an alternate to the compressible flow equation with the momentum flux term for modeling multidimensional geometries. An alternate form of the momentum equation developed by Zuber[23] is obtained by using a different control volume approach yielding the compressible integral momentum equation (Form 4).

Heat Transfer Model. The transfer of thermal energy between the fluid and the boundaries is modeled by a combination of transient conduction and convective heat transfer correlations. The thermal interactions that are modeled in this way include reactor fuel pin to fluid, steam generator primary fluid to wall to secondary fluid, and vessel/piping system stored energy to fluid. Models also exist for internal heat generation in the wall or fluid due to electrical or gamma heating. The transient conduction is calculated using a Crank-Nickolson finite difference technique for the one-dimensional transient heat conduction equation.[24] Slab, cylindrical, or spherical geometry can be represented. The geometry and conditions of the heat conductor are specified by the user.

The convective heat transfer at fluid boundary interfaces is the boundary condition for the transient conduction solution and is the source or sink of thermal energy to the fluid. The code uses convective heat transfer correlations to calculate the critical heat flux (CHF), pre-CHF heat transfer, and post-CHF heat transfer. The basic approach used in RELAP4/MOD6 is to construct a heat transfer surface for the wall heat flux as a function of the wall superheat and fluid quality. This heat flux surface is constructed from a variety of correlations for different ranges of the independent variables. In general, it is necessary to represent a wide range of conditions from subcooled liquid forced convection to two-phase film boiling. The details of this subject are discussed in other chapters. The users manual for a particular code version of interest should be consulted for specific information on the correlations used.

Component Models. The hydrodynamic and heat transfer models are quite general and can be applied to any thermal-fluid system (within limits established by the basic assumptions). However, there are several models that are specific to certain components such as pumps, jet pumps, fuel rods, valves, controls, etc. These are briefly described in the following.

Both the quasi-steady hydrodynamic performance and the transient operation of a centrifugal pump are modeled. The quasi-steady performance is modeled using emperically established homologous curves that relate the centrifugal pump similarity parameters for single-phase operation. From these curves any one of the parameters (head, volumetric flow, or speed) can be established from the remaining two. Pump performance under two-phase conditions is modeled using a head degradation parameter, which is a function of the pumped

fluid void fraction. The transient mechanical operation of the pump is modeled by applying the angular acceleration relation for the pump and motor. The motor power is variable to enable pump trip and coastdown to be simulated.

For jet pumps, the momentum exchange between the drive flow and the pumped fluid is modeled using a special form of the momentum equation that includes the mixing effect of multiple streams at different velocities. Discontinuities that occur upon flow reversal are smoothed.

The fuel model consists of a space independent model for the fission- and radioactive-decay energy generation processes. The model includes reactivity feedback effects from the fuel temperature, water density, and water temperatures. The kinetics equations are solved using a numerical method similar to the IREKIN[25] code. The thermal energy generated in the fuel is transferred to the coolant by means of conduction through the ceramic fuel pellet, across the interface/gap between the fuel and the clad, and finally, across the clad. The conduction through the fuel pellet and the clad can be accurately characterized, but the conduction across the fuel/clad interface requires greater detail. The gap dimension varies with fuel and clad temperature and even when the fuel and clad are in contact, there remains a significant resistance. A dynamic fuel model is included for establishing the gap resistance due to change in the gap dimensions and change in pressure of the gas within the gap. Several other phenomena such as axial fuel/clad expansion, fuel/clad swelling, and metal-water reaction are also considered in the fuel model.[26]

On/off and check-valve models are included. The on/off valve is activated by a logical test on one or a combination of system variables such as time, pressure, temperature, etc. The check-valve model can include the effect of fluid forces and the inertia of the poppet.

Control functions can be simulated by means of logical trips using time or any system parameters. The action that can be taken includes reactor scram, open/close valves, motors on/off, and even some change to the models that are employed for a period of operation.

Solution Method. The basic numerical scheme used in RELAP4/MOD6 and MOD7 is essentially the same as the original scheme developed for the FLASH4 code.[27] The approach consists of expressing the pressure in each control volume in terms of the corresponding mass and energy that exist in the volume at the end of a finite time interval. The expressions thus obtained for the pressures are in terms of the junction mass and energy fluxes so that substitution of these expressions into the momentum or flow equations at the appropriate junctions results in a system of coupled linear difference equations for the junctions flows. The coupling for a system of consecutive control volumes is such that a tridiagonal matrix of linear equations in the new time junction flows is obtained.

When branches or cross connections are present, the solution matrix is no longer tridiagonal. Thus the general solution scheme for the system of equations consists of a reduction algorithm by which the tridiagonal portions of the matrix are reduced directly followed by inversion of the reduced matrix. The matrix inversion can be accomplished by direct or iterative methods. The RELAP4/MOD6 solution scheme uses a direct matrix solver for small systems, less than 14 volumes, and an iterative scheme for large systems. When the iterative solution scheme is used, the time step must be small enough to obtain a diagonally dominant matrix.

Once the solution for the junction flows is obtained, the remaining variables such as control volume mass, energy, pressure, etc., are obtained by back substitution into the respective conservation equations and use of the constitutive relations (equation-of-state, wall friction, heat transfer, etc.).

Programming. The RELAP4 program is written in FORTRAN IV, and the MOD5 and MOD6 versions are operable on both the IBM-360 and CDC-7600 computers; while the MOD7 version is only operable on the CDC-7600 and -176 series computers. The running time of a RELAP4/MOD6 loss-of-coolant problem can vary from minutes to hours, depending primarily upon the number of fluid volumes used, the coolant break size, and the number of heat conduction nodes used throughout a given system representation. For LWR models ranging from 15 to 40 fluid volumes, running time through refill may range from 15 to 60 minutes or more on the CDC-7600 and from 2 to 8 hours or more on the IBM-360/75.

3.4 RELAP4 Example Calculations

The RELAP4/MOD6 code has been used extensively in integral system simulations for some time, and for this reason, we will present results for one integral experiment. The example is a recent Semiscale Mod-3 test, S-07-6, which was included in the assessment effort on RELAP4/MOD6.[28] This experiment has also been modeled using RELAP5 and thus serves as a basis for comparison of the relative performance of the codes.

Mod-3 designates the latest major hardware modifications in the Semiscale Test Facility. Whereas early Semiscale testing was directed toward Loss-of-Fluid Test Facility (LOFT) counterpart and blowdown heat transfer experiments, Mod-3 was designed to model LOCA behavior in PWRs more easily.[29] The Mod-3 system differs from the previously operated Mod-1 system in three important aspects. First, Mod-3 has a new vessel that contains a full-length (3.66-m) heated core, has a full-length upper plenum and upper head with internal structures representative of those in a full-sized PWR with upper-head injection (UHI), and has an external downcomer. Second, an active pump and an active steam generator have been added to the broken loop. Third, the break simulation has the capability to represent communicative breaks of various sizes. Fig. 1 is an isometric sketch of the Mod-3 facility showing the most important features.

Test S-07-6 was the first integral blowdown and reflood experiment to be performed in the Mod-3 system. The test was a 200% cold-leg break with cold-leg ECC injection. A complete set of initial and operating conditions for this test is given in Ref. 30.

RELAP4/MOD6 Model for Semiscale Mod-3 Test S-07-6. Two RELAP4/MOD6 models were used to predict the behavior of Test S-07-6.[28] A blowdown model was used to calculate the transient response from the time of the simulated piping break until the end of the lower-plenum refill. A separate reflood model was used to model the reflood period through rod quench.

The model nodalization diagram used in the analysis of the blowdown and refill phases is shown in Fig. 2. The model includes 52 control volumes and 67 junctions. One control volume is used to represent the lower plenum, one the core mixer box, and two sets of 5 volumes for the hot and average channels in the core. The inlet annulus, guide tube, support tubes, and the upper head are each represented by one volume. The downcomer and upper plenum are each represented by three volumes.

A total of 50 heat slabs was used to represent heat conducting solids in contact with the coolant in the core, downcomer, steam generators, vessel, and piping. The high-power rods in the core are represented by 12 axially-stacked heat slabs, and the low-power rods are similarly represented by 5 heat slabs.

The heat transfer correlations used in the calculation are highly influential in determining the core thermal and hydraulic response. In this pretest prediction, the set of RELAP4 heat transfer correlations designated HTS2 was used. The heat transfer correlations as they are applied in specific regions of the boiling curve are tabulated in Table III.

The vertical-slip option was used in all downcomer, core-, guide- and support-tube junctions. The bubble-rise option was used in the following locations: (1) intact- and broken-loop accumulators, (2) the pressurizer, (3) the intact- and broken-loop steam-generator secondaries, (4) the pressure suppression tank, and (5) the upper head. The bubble-rise model was used in the upper and lower plenum, to be consistent with the use of the slip model in the core.

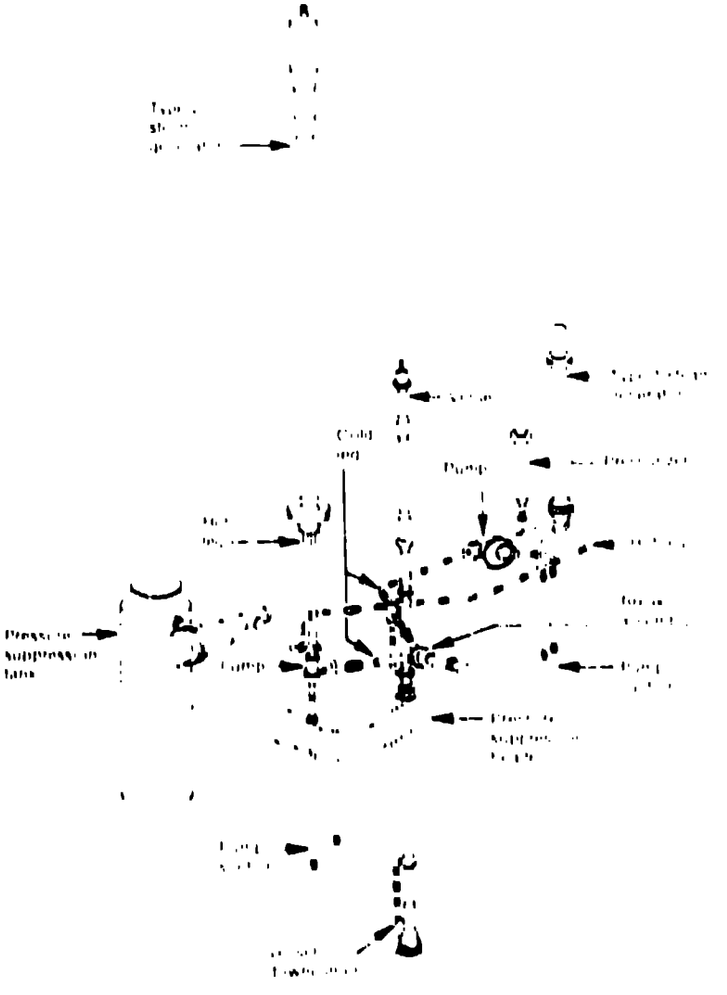

Fig. 1. Isometric sketch of the Semiscale Mod-3 Facility.

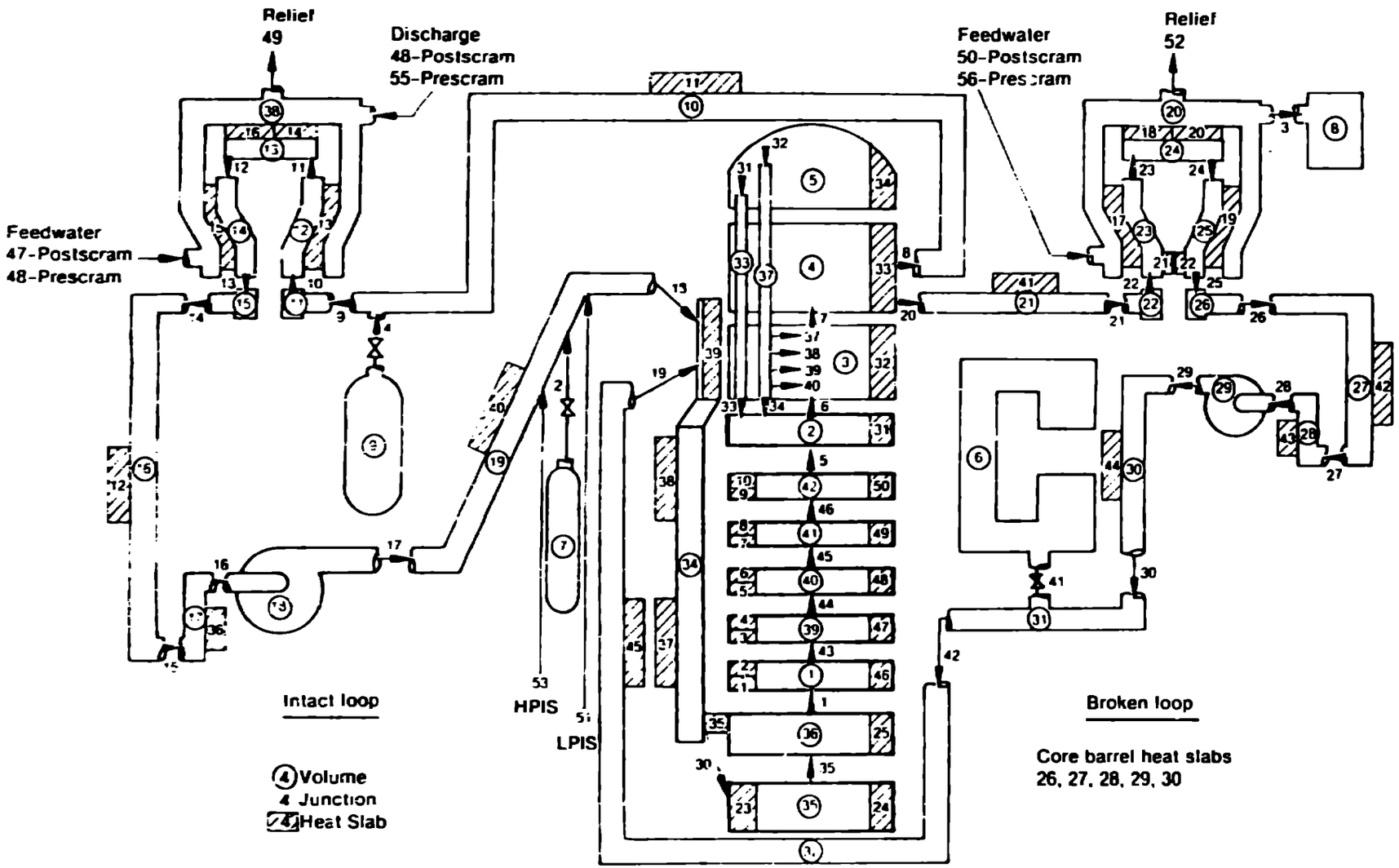

Fig. 3. PELAN 4 blowdown nodalization, Mod-3 Test S-07-6.

TABLE III

RELAP4/MOD6 HEAT-TRANSFER CORRELATIONS, TEST S-07-6

Region	Correlation
Subcooled forced convection	Dittus Boelter
Saturated nucleate boiling	Chen
Subcooled nucleate boiling	Modified Chen
High-flow transition boiling	Modified Ton-Young
High-flow film boiling	Condie-Bengston
Forced convection to vapor	Dittus-Boelter
Low flow, low void fraction	Hsu and Bromley-Pomeranz

The critical-flow model used was the Henry-Fauske/Homogeneous Equilibrium model (HF/HEM). A multiplier of 0.84 was used with the HEM for saturated blowdown and 1.0 was used with the subcooled and saturated HF critical-flow model. The transition quality was set to the default value of 0.02. The break nozzles are modeled as Junctions 26 and 27.

Reflood Analysis Model. The nodalization diagram for the model used to analyze the reflood portion is similar to that for the blowdown portion, shown in Fig. 2, but with the following differences. The downcomer is modeled by two fluid volumes rather than the four volumes used during blowdown. The pressurizer volume was discarded to reduce computer running time since the pressurizer empties during blowdown. Further nodalization changes include fewer volumes in piping, plena, and the steam-generator primary side.

The incompressible momentum equation form that excludes momentum-flux terms was used for the reflood analysis, i.e., kinetic terms were assumed to be small. Phase separation was modeled in the upper plenum and in the two downcomer volumes. For the upper plenum, the Wilson bubble-rise model was used. Complete phase separation was assumed for the downcomer volumes.

Initial conditions for the reflood analysis were taken from the blowdown analysis at the calculated end of lower plenum refill. Because the nodalization was different for the two analyses, an attempt was made to preserve fluid quality in regions that were lumped together. Heater rod temperatures were reinitialized at current fluid temperatures. ECC injection was specified by extrapolating calculated ECC behavior from blowdown through accumulator emptying and continuing the low-pressure injection.

Principal performance evaluators for the blowdown transient are system pressure for hydraulic processes and hot-channel cladding temperature histories for thermal response. An important diagnostic indicator is the density fluid in the lower plenum. Figure 3 shows a comparison of system pressure between calculation and experiment. The agreement is adequate until about 13 s into the transient. After that the calculated depressurization rate is greater than the measured rate and the experimental end of blowdown lags the calculated time by about 15 s. Thus, the analysis shows the end of the refill period to be at about 45 s, whereas in the experiment, this event occurs after 50 s. The cladding temperature history in the hot channel (Fig. 4) indicates an underprediction of the maximum temperature by as much as 75 K.

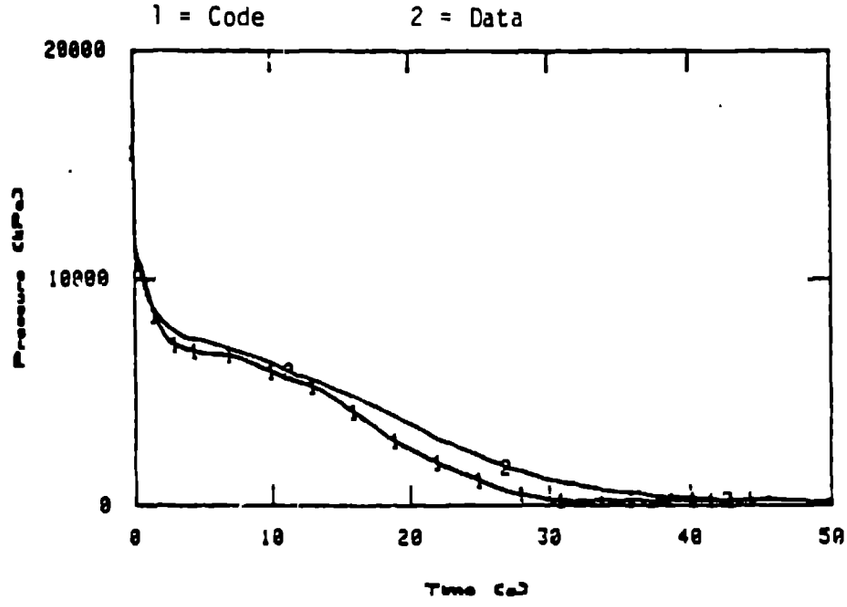

Fig. 3. System pressure history for Test S-07-6 blowdown.

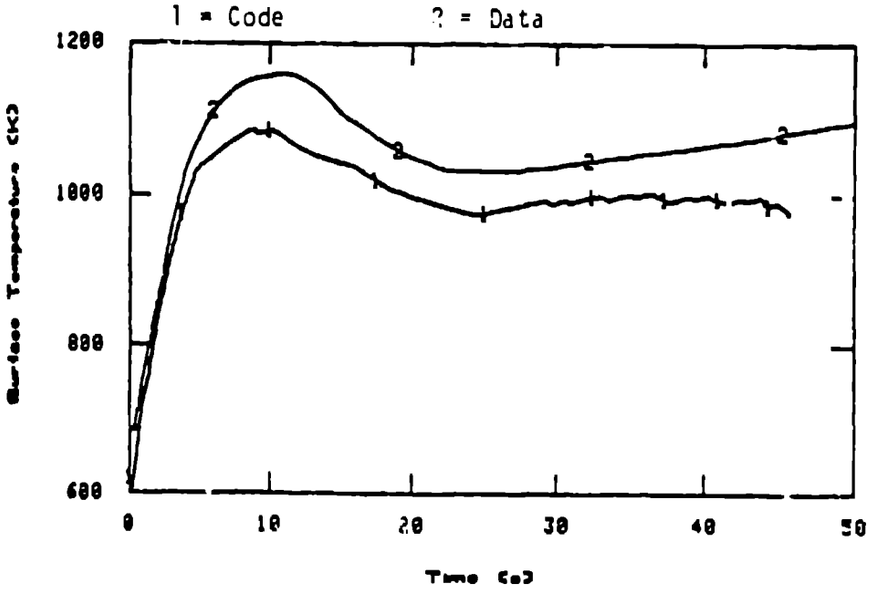

Fig. 4. Cladding surface temperature at the 1.84-m elevation in the hot channel for Test S-07-6 blow down.

Reflood Calculations and Data Comparisons. The reflood phase was considered to start at 45 s into the transient. This was the calculated time-to-lower-plenum refill. During reflood, the maximum cladding temperature, time to temperature turnaround, and time-to-rod quench are normally considered to be important performance evaluators. Parameters such as the downcomer liquid level, core liquid level, and core inlet density are considered diagnostic indicators.

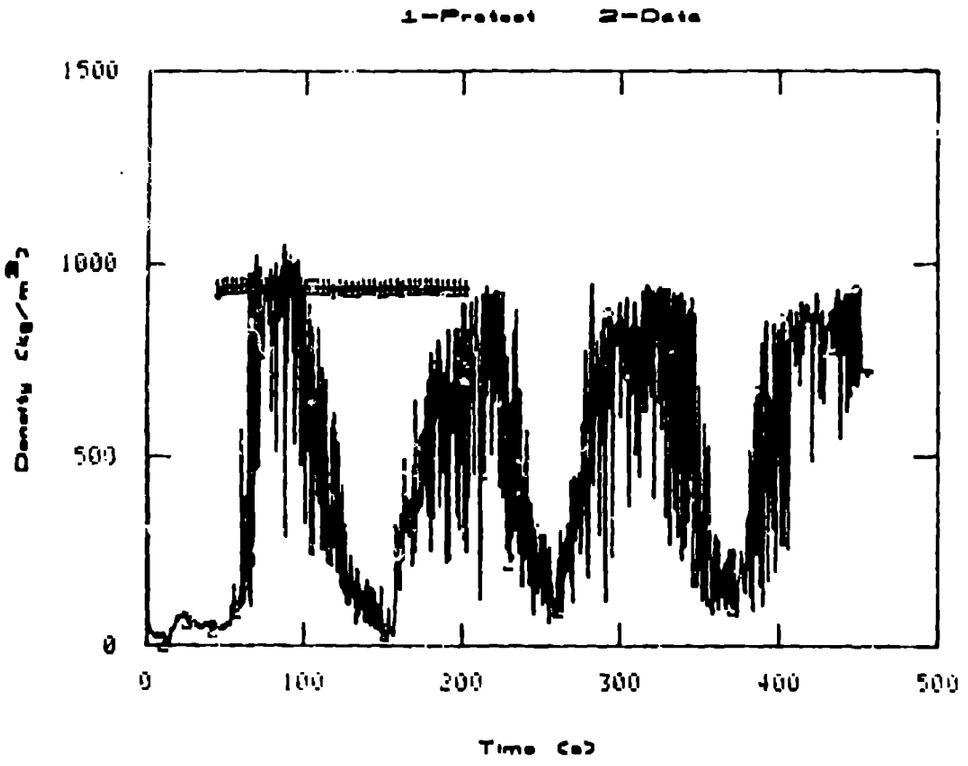

Fig. 5. Calculated and measured core inlet density, Test S-07-6 reflood.

Figure 5 shows the core inlet density as calculated and measured. The measurement shows a voiding of the core at about 100 s, followed by a long-period oscillation in the inlet flow. The calculation indicates that the fluid at the core inlet remains a dense liquid. The observed downcomer voiding also followed the pattern of core inlet density, whereas the calculation shows the downcomer to remain liquid-filled.

The base-case code-data comparisons demonstrated a need for incorporating mechanisms of liquid voiding in the modeling of the Semiscale Mod-3 downcomer. A primary contributor to this voiding behavior was determined, on posttest review, to be extensive vapor generation attributable to unanticipated heat transfer from the downcomer wall to the fluid. An additional study was made, incorporating wall heat transfer in the analysis and providing some facility for voiding downcomer liquid by changing to a Wilson bubble-rise model in the downcomer volumes. The results of the study indicated a tendency to improve but failed to provide acceptable code-data agreement.

Temperature histories are shown in Fig. 6 for the cladding at a location approximately at core midplane. The measured temperature is compared with the results of both the base-case analysis and the revised analysis. When voiding first occurs at about 100 s, both analysis and measurement (Fig. 6) show a tendency for the temperature to decrease as the core outlet flow also decreases. This decrease is followed by a slight temperature rise in the revised calculation and a major rise in the measured temperature--the difference being attributable to the failure of the calculation to sustain the voiding characteristic.

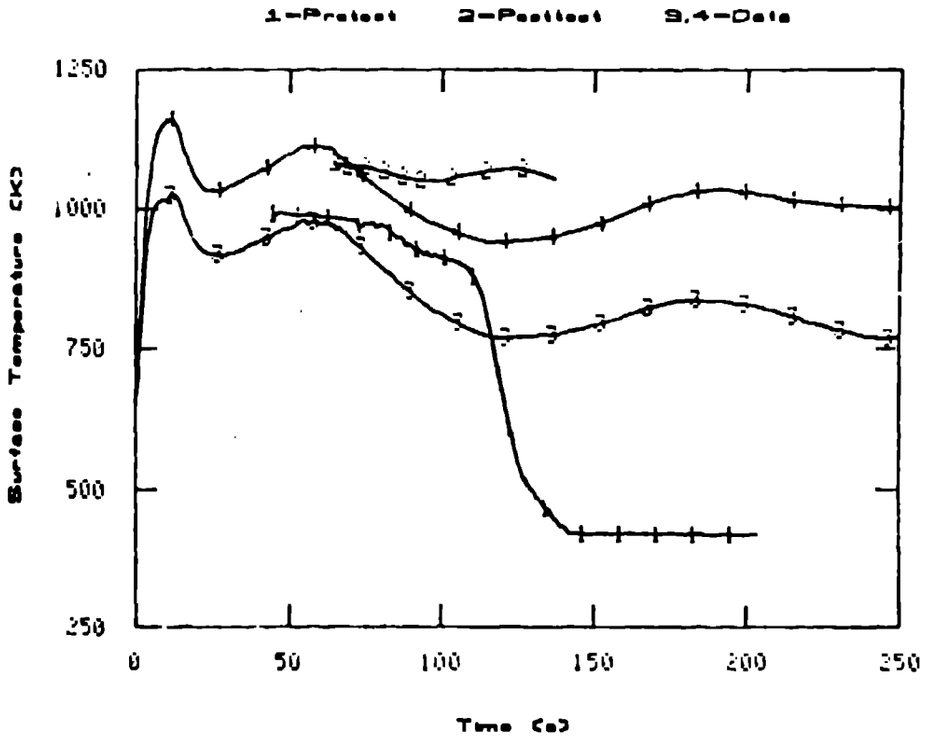

Fig. 6. Cladding surface temperature at the 1.84-m elevation in the hot channel for Test S-07-6 with additional calculation.

4. RELAP5 DESCRIPTION AND EXAMPLE COMPUTATIONS

The RELAP5 development objective[8] is an economical and user-convenient code for system transient simulation of LWR LOCA and non-LOCA transients. RELAP5 is an advanced, one-dimensional, fast-running system analysis code. It is a completely new code based on a nonhomogeneous, nonequlibrium hydrodynamic model and features top-down structural design with the significant programming elements coupled in modular fashion. To a great extent, the development of RELAP5 has been influenced by the experience gained through the development and usage of the RELAP4 series of codes. This is evident in the emphasis placed on the convenience with which both the developer and the user can interface with the code.

The RELAP5 code includes the thermal-hydraulic and mechanical models used to describe the processes that occur during transient operation and postulated accidents in an LWR. Component process models are included for pipes, branches, abrupt flow area changes, pumps, accumulator, valves, plant trips, heat transfer, neutronics, and choked flow. These, as well as other models, have been integrated into a versatile system code framework.

4.1 Program Status

The RELAP5 code is now operational, has been tested on hypothetical problems as well as actual experimental systems, and is in use at the Idaho National Engineering Laboratory for pre and posttest predictions of the LOFT, Semiscale and PBF experiments. The first version, RELAP5/MOD0, is available from the

National Energy Software Center at Argonne National Laboratory. A code description and user's manual are also available. All the discussion and example computations presented herein refer to this version that was developed for modeling the blowdown portion of an LWR LOCA. Development of RELAP5 is continuing, and a new version will be completed during 1980 that includes an accumulator model, point neutronics, a noncondensible component of the vapor phase, small-break stratification models, improved heat transfer models, and faster running capability.

4.3 Model Description

Hydrodynamic Model. The hydrodynamic model developed for the RELAP5 code[31-33] includes the important physics of the two-phase-flow process, while incorporating any simplifying assumptions consistent with the end use of the model. The principal simplification is that one of the phases exists at the saturation state. Generally, it is sufficient to specify that the least massive phase be at saturation, i.e., the phase that is either appearing or disappearing. The specification of one phase temperature greatly reduces the amount of constitutive information that must be provided relative to interphase and overall energy transfer. All interphase energy transfer mechanisms are implicitly lumped in the vapor mass generation model. Thus, a single correlation replaces the need for constitutive relations for interphase energy transfer, distribution of external energy transfer between phases, and distribution of energy transfer between sensible heat and heat of vaporization. In addition, only a single overall energy equation is required.

The two-fluid nonequilibrium hydrodynamic model includes options for simpler hydrodynamic models. Included are a homogeneous flow model and/or a thermal equilibrium model. The two-fluid or homogeneous flow models can be used with either the nonequilibrium or equilibrium thermal models, i.e., four combinations. The primary reason for inclusion of the homogeneous/equilibrium option is to permit the code to be compared to existing HEM code results such as RELAP4 for the purpose of checkout and development.

Field Equations. The basic field equations[34] for the two-fluid nonequilibrium model consist of the two phasic continuity equations, the two phasic momentum equations, and the mixture total energy equation--a total of five equations. The equations are employed in stream-tube differential form with time and one space dimension as independent variables and in terms of dependent variables, which are time- and volume-averaged quantities. The phasic mass conservation equations are summed and differenced to obtain a mixture continuity equation and an equation for the temporal variation of the mixture quality.

The phasic momentum equations are also used as a sum and difference. The sum equation is obtained by direct summation of the phasic momentum equations with the interface conditions substituted where appropriate. The difference of the phasic momentum equations is obtained by first dividing the vapor and liquid phasic momentum equations by the respective product of phasic void fraction and density and, subsequently, subtracting. Here again, the interface momentum conditions are employed.

The mixture total energy equation is obtained by summing the phasic energy equations. This mixture equation is transformed into the equivalent thermal energy equation by using the momentum equations to obtain a mechanical energy equation, which is subsequently subtracted from the total energy equation. Here again the interface conditions are employed to simplify the resulting energy equation. The reason for selecting the thermal energy

equation rather than the total energy equation is that the development of the numerical scheme is simplified. The thermal energy equation does not involve time derivatives of the kinetic energy and thus fewer new time variables will appear in the approximate finite difference equations.

State Relations. The dependent variables that appear as temporal and/or spatial derivatives in the five field equations are density, pressure, static quality, mixture internal energy, and the two phasic velocities. The phasic properties also appear in the spatial derivatives and as coefficients of the derivatives. To obtain a determinant system, the state relationship must be employed wherein density and the phasic properties are expressed as functions of the pressure, static quality, and mixture internal energy. The state of the system is established from this information and from the specification that one of the phases exists at the prevailing saturation condition.

The state of each phase is established by specification of the pressure and phasic internal energy (only the pressure is needed to specify the state of the saturated phase). For the case of subcooled liquid or superheated vapor, these states are established using tabular equilibrium data as a function of the pressure and phasic internal energy. For the pseudo states of superheated liquid and subcooled steam, the properties are extrapolated along isobars using property derivatives evaluated at the corresponding saturation state.

In addition to the state properties, derivatives of the mixture density with respect to the pressure, static quality, and mixture internal energy are required in the numerical solution scheme. These derivatives can be expressed in terms of the isothermal compressibility and the isobaric coefficient of thermal expansion, both of which are available from the state properties data.

Constitutiv Relations. A primary feature of the RELAP5 hydrodynamic model is that only two basic interphase constitutive relations are required, i.e., interphase mass transfer and interphase drag. The specification that one phase exists at local saturation conditions replaces the need for energy transfer and partitioning constitutive relations, both between phases and between each phase and the wall. The only heat transfer correlation required is the overall wall-to-fluid correlation. The RELAP4/MOD6[18] convective heat transfer correlations are used for this purpose. The remaining required constitutive relation is for wall friction. Here again, an existing two-phase multiplier correlation has been adapted.[18]

In summary, four constitutive relations are required by the hydrodynamic model--the vapor generation rate, the interphase drag, the wall friction, and the wall heat transfer. These relations are primarily empirical in nature as opposed to the field equations that characterize the fluid dynamic behavior. However, the ability of any numerical hydrodynamic model to agree with or predict physical phenomena with accuracy will depend heavily on the accuracy of the constitutive relations.

The vapor generation rate is the result of several mechanisms such as interphase energy transfer rate, the energy partitioning between phase change and sensible heat, interphase surface area, nucleation site density, turbulence level, etc. In RELAP5, all of these separate but interacting mechanisms are modeled by a single dimensionless correlation. This vapor generation model was developed by merging the results of three independent and widely varying investigations. The three approaches are (1) a mechanistic model by Jones and Saha[35] based on interphase energy exchange, (2) an empirical dimensional correlation by Houdayer, et al.,[36] from the Moby Dick

data, and (3) the results of a dimensional analysis to establish the dimensionless groups and functional form of the vapor generation rate. The last of these efforts was completed as a part of the RELAP5 project[3] in order to establish the scale dependence of the vapor generation function.

Interphase drag consists of two parts--the dynamic drag due to the virtual mass acceleration and the steady drag arising from viscous shear between phases. The dynamic drag has been included because of the effect it has on the sound speed and hence, the choking criterion. The dynamic drag is calculated based on the induced mass of a spherical bubble (or drop) in a mixture of vapor bubbles (or liquid drops) and liquid or vapor). The steady drag depends on the flow regime and the relative phase velocity.

The flow regime map used in RELAP5 is a simplified Bennett map[37] for vertical flow and is similar to the one used by TRAC.[8] The flow regimes are classified into the general categories of dispersed, separated, churn turbulent, and transitional flow.

Constitutive relations for the steady drag are formulated for the separated and dispersed flows based on semimechanistic models. The drag in the transition regimes is calculated by linear interpolation on the reciprocal values of the separated or dispersed-flow drag coefficients defined at the boundaries of the particular transition region. This yields a continuous variation in the calculated relative velocity. The calculation of the drag due to the virtual mass effect is based on an objective and symmetric formulation of the relative acceleration proposed by Lahey.[38] This formulation involves spatial and temporal derivatives of the phase velocities with a correlation for the virtual mass coefficient of Zuber's.[39]

The wall friction force terms only include wall shear effects. Form losses due to abrupt area change are calculated using mechanistic form-loss models. Other form losses due to elbows or complicated flow passage geometry are modeled by specified energy loss coefficients. Wall shear losses in piping systems are usually small compared to form losses, thus a relatively simple approach that yields an accurate steady-state frictional pressure drop is employed.

The HTFS modification of the Baroczy two-phase friction multiplier correlation[40] was used with the Colebrook correlation for the single phase friction factor including wall roughness effects. Both laminar and turbulent flow regimes are included. The two-fluid hydrodynamic model requires that the wall friction force be partitioned between the liquid and vapor phases. The method used in RELAP5 is based on void fraction partitioning of the friction force. The phasic friction components are normalized so that the sum of the phasic frictional forces agrees with that derived from the two-phase multiplier approach.

Heat Transfer Correlations. The wall heat transfer correlations used in RELAP5/MOD0 are adaptations of the blowdown heat transfer package from RELAP4/MOD6.[18] In adapting the RELAP4 package, the correlations were converted to scientific notation units and only the Condie-Bengston correlations were retained for use in the transition and film boiling regions. In addition, the procedure for applying correlations was modified to eliminate the need for iteration and to allow the same procedure to be usable for both steady-state and transient calculations.

Special Process Models. Special models are used in RELAP5 for those processes that have small relaxation times or are so complex in nature that they must be modeled by quasi-steady empirical models. Break flow, internal choking, abrupt area change, and branching are examples of processes having short relaxation times compared to component transport times. The hydrodynamic performance of pumps and valves are examples of processes that are too complex to be modeled from first principles, so empirical correlations are used. The use of quasi-steady models for break flow and flow at abrupt area changes results in considerable computer time savings since it eliminates the need for fine nodalization at such points.

A break flow model[41,42] is included for calculation of the mass discharge from the system at such points as a pipe break or a nozzle in the case of scaled experiments like Semiscale or LOFT. Generally, the flow at such breaks is choked until the system pressure nears the containment pressure. The RELAP5 break flow model is used to predict the flow at such system discharge points and is also used to predict and calculate choked flow at internal points in the system. The model is based on characteristic theory in which a criterion is developed for the conditions under which propagation of pressure signals upstream just ceases. This theory applies to all two-phase conditions. Additional theoretical considerations have been employed to extend the break flow model to conditions of subcooled liquid flow that flashes at the point of mass discharge.

The general reactor system contains piping networks that consist of many sudden area changes and orifices. In order to apply more efficiently the hydrodynamic model to such systems, analytical models for these components have been developed.[43] The RELAP5 abrupt-area-change model is based on the Bourda-Carnot[44] formulation for a sudden enlargement and standard pipe flow relations, including vena-contracta effect, for sudden contractions and/or orifices. Quasi-steady continuity and momentum balances are employed at points of abrupt area change. The numerical implementation of these balances is such that the hydrodynamic losses are independent of the upstream and the downstream nodalization. In effect, the quasi-steady balances are employed as jump conditions that couple fluid components having abrupt change in cross-sectional area. This coupling process is achieved without change to the basic linear semi-implicit numerical time-advancement scheme.

In order to model flow in interconnected piping networks, it is necessary to model the two-phase fluid process at tees, wyes, and plenums. A general description of the two-phase flow process is complicated by the possibility of phase separation effects.[45] However, there are many situations where wye or plenum branching is adequate for both flow merging and division. Typical situations are parallel flow paths through the reactor core, jet pump flow mixing sections, and any branch from a vessel of large cross section (in this case the fluid momentum is small and it is entirely permissible to neglect the momentum convective terms). For branching situations where phase separation effects due to momentum and/or body force effects are important, a branching algorithm has been developed[7] in which the parallel or wye branching model is used to map the two-dimensional situation onto the one-dimensional space of the fluid model.

The RELAP5 pump model is a straightforward conversion of the RELAP4 centrifugal pump model.[17] The pump is interfaced to the unequal velocity hydrodynamic model of RELAP5 quite simply by assuming that the head developed by the pump is similar to a body force term that appears only in the mixture

momentum equation. The pump dissipation term for the thermal energy equation is computed from the total pump power (given by torque times rotational speed) minus the rate of fluid reversible energy addition.

Numerical Methods. The RELAP5 numerical solution scheme[34] is based on replacing the system of differential equations with a system of finite difference equations, which are partially implicit in time. In all cases, the implicit terms are formulated to produce a linear time advancement matrix, which is solved by direct inversion using a sparse matrix algorithm. An additional feature of the scheme is that the implicitness has been selected such that the five field equations can be reduced to a single difference equation per fluid control volume or mesh cell in terms of the hydrodynamic pressure. Thus, only an NxN system of difference equations must be solved simultaneously at each time step. (N i the total number of control volumes used to simulate the fluid system.)

The difference equations are based on the concept of a control volume or "mesh cell" in which mass and energy are conserved by equating accumulation to rate of influx through the cell boundaries. This results in defining mass and energy volume average properties and requiring knowledge of velocities at the volume inlets and outlets (junctions). The junction velocities are conveniently defined through use of momentum control volumes that are centered on the mass and energy cell inlets and outlets. This produces a numerical scheme having a staggered spatial mesh. The scaler properties (pressure, energy, and quality) of the flow are defined at cell centers and vector quantities (velocities) are defined at the cell junctions. The resulting one-dimensional spatial noding is illustrated in Fig. 7. The term cell is used throughout the discussion to mean an increment in the spatial variable corresponding to the mass and energy control volume.

The mass and energy difference equations for each cell are obtained by integrating the stream-tube formulations for the mass and energy equations with respect to the spatial variable, x, from the junction at x_j to x_{j+1}. The momentum equations, on the other hand, are integrated with respect to the spatial variable from cell center to adjoining cell center (x_K to x_L) as seen in Fig. 7. In all cases, the correlation coefficents for averaged products are taken as unity so that averaged products are replaced directly with products of averages.

Several general guidelines were followed in developing the overall numerical scheme. These guidelines are summarized below.

1. Mass and energy inventories are very important quantities in water reactor safety analysis and as such the numerical scheme should be consistent and conservative in these quantities (a greater degree of approximation for momentum effects was considered acceptable). Both mass and energy are convected from the same cell and each is evaluated at the same time level (i.e., mass density is evaluated at old time level so energy density is also evaluated at old time).

2. In order to achieve fast execution speed, implicit evaluation is used only for those terms necessary for numerical stability, elimination of the wave propagation time-step limit, and those phenomena known to have small time constants. Thus, implicit evaluation is used for the velocity in mass and energy transport terms, the pressure gradient in the momentum equations, and the interphase mass and momentum exchange terms.

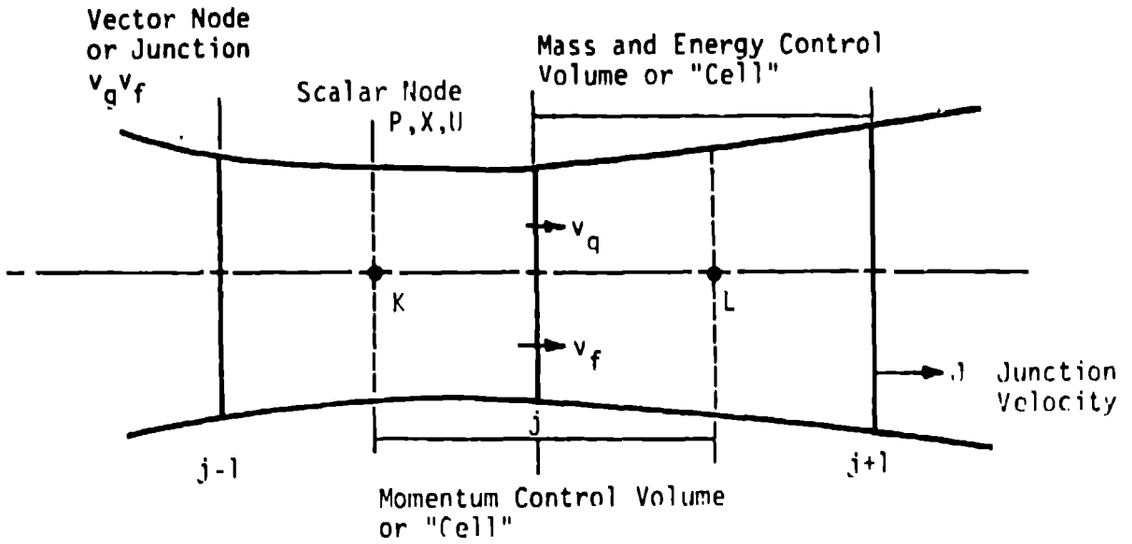

Fig. 7. Difference equation nodalization schematic.

3. To further enhance computing speed, the time level evalutions were selected so that the resulting implicit terms are linear in the new time variables. Where it was necessary to retain nonlinearities, two term Taylor series expansions about old time values were used to obtain a formulation linear in the new time variables (higher order terms were neglected). High computing speed is achieved by eliminating the need to solve large systems of nonlinear equations iteratively.

A well-posed numerical problem is obtained as the result of several factors. These include the selective use of implicitness (evaluation of spatial gradient terms at the new time), donor formulations for the mass and energy flux terms and use of a "donor-like" formulation for the momentum flux terms. The well-posed final numerical scheme (as well as its accuracy) has been demonstrated by extensive numerical testing during development.

System Code Development. The primary emphasis in the system code design of RELAP5 has been to achieve an economical code. Attention has been focused on reducing computer time per mesh point per advancement. Time step control algorithms have been included to minimize the number of advancements. Dynamic storage has been used to keep the computer memory requirements to a minimum.

The user's time in setting up, debugging, and interpreting results is also significant. User conveniences significantly reduce overall simulation costs. The system code includes many modeling disciplines such as hydrodynamics, pumps, valve actions, heat transfer, and neutronics. Because the details of the system must be described to the program, the requirement for a large amount of data cannot be avoided. Thus, user-oriented input, extensive error checking, and several forms of printed and plotted output are provided.

Experience gained from the development and use of RELAP4 has shown that to achieve true economy, the code structure must provide for ease of addition and modification. Care has been taken in RELAP5 to structure data files and program organization in a modular fashion in order to achieve this goal.

The RELAP5 code is organized into four basic parts: input, steady-state initialization, transient calculations, and the output functions. Each of these parts is summarized in the following.

The code contains extensive input processing routines designed to help the user find input errors and in a small number of checkout runs to obtain an error-free input data deck. The input processor is designed to process all input for every job submitted and to list the errors. In this respect the input routine is similar to a FORTRAN complier. The error-checking routines find impossible or conflicting data specifications and misapplications of the various models. The input routines also process program control data for such functions as major/minor edits, writing of restart records, and creation of plot files.

The steady-state portion of the code is intended to produce the initial conditions for starting transient calculations. This capability is currently incomplete, and the input and generalized restart features are used to provide this function. The initial conditions can be input, or a transient calculation can be made to achieve a steady state and then the generalized restart feature is used to modify the configuration and initiate the transient. Transient hydrodynamic, heat transfer, and neutronics calculations are performed in the transient portion of the code. Other functions are time-step regulations and trip logic calculations.

The output portion of RELAP5 provides both major and minor output edits at specified intervals, prepares restart records, and generates plot files for graphical output. RELAP5 has an internal plotting feature for graphical output, and can also be used with any external plotting package. Internal diagnostic edits are provided whenever the code fails due to water property errors, which are generally symptomatic of an unrealistic modeling condition.

4.4 RELAP5 Example Calculations

The RELAP5 code has been used to model several separate-effects experiments and some limited system experiments. The separate effects experiments that have been modeled include the Edwards 3-inch[46] and 8-inch pipe blowdowns; the Edwards Phase II two-pipe blowdown; the Moby Dick Run 447; the General Electric one-foot vessel level swell; the Marviken III Tests 4,[42] 22, and 24; Semiscale Tests Mod-2 S-01-4a, Mod-2 S-06-2, and Mod-3 S-07-6;[47] and the LOFT Tests L3-0, L3-1, and L3-2. These tests have been used for developmental assessment. In all cases the performance achieved using the code has been good. The LOFT system test simulations are the most recent applications of the code and good agreement with data was achieved while requiring a CPU time less than real time for the L3-2 experiment prepediction.

Three representative applications of the code that will be summarized in the following discussion are the Marviken III Test 4, the Semiscale Mod-3 Test S-07-6, and the LOFT LOCE L3-2 small-break test.

Marviken III Test 4. The RELAP5 code was used to simulate the Marviken III Test 4[42] to evaluate the code's ability to predict the hydrodynamic behavior of a large-scale blowdown test. Simulation of the test allows evaluation of the choked flow model under conditions that are comparable to those expected in an LWR during a postulated LOCA.

The purpose of the Marviken III Test 4* was to establish choked flow rate data for a large scale nozzle (500 mm in diameter) with subcooled and low-quality water conditions at the nozzle inlet. A schematic of the pressure vessel, discharge pipe, and test nozzle is shown in Fig. 8. The pressure vessel was initially filled with water to an elevation of 16.8 m above the discharge pipe inlet. The steam dome above the water level was saturated at 4.94 MPa. The water level was at nearly saturation conditions for about 6 m below. The water was subcooled by about 30 K below the saturated fluid after a small transition zone. The initial temperature profile is also shown in Fig. 8.

The nodalization used for the numerical simulation is also illustrated in Fig. 8. A nearly uniform cell length of about 1 m was used everywhere. No special nodalization was used in the nozzle region. This was possible because RELAP5 includes an analytical choking criterion that is applied at the throat of the nozzle.

The calculated blowdown transient was simulated by opening the discharge pipe outlet to the ambient pressure. The measured data consisted of pressures, differential pressures, temperatures, and mass discharge rates inferred from pitot-static pressure data. Corresponding values were calculated and comparisons are shown in Figs. 9 and 10. Figure 9 shows the pressure history at the vessel top. Except for an initial nonequilibrium undershoot (at about 3 s after rupture), the depressurization process was essentially in equilibrium. The calculated blowdown rate was in agreement with the system blowdown rate, and since the depressurization rate was controlled by the break mass flow, the fact that the pressure profiles were in agreement demonstrates that the discharge flow was modeled accurately.

A comparison of the calculated and inferred discharge flow rates is shown in Fig. 10. The clear transition from subcooled to two-phase critical flow is shown both in the test data and in the calculations at about 17 to 20 s after rupture. This was reflected in the numerical calculations as the code automatically switched from the subcooled choked-flow criterion to the two-phase criterion.[42]

Comparison of the RELAP5 calculations with the Marviken III Test 4 results provides a good evaluation of the ability of a two-phase thermal-hydraulic model to predict mass discharge rates correctly under choked-flow conditions at large scale.

Semiscale Mod-3 Test S-07-6. The Semiscale Mod-3 system[29] and a summary of the Test S-07-6[30] are given as a part of the RELAP4 modeling of this same test. The application of RELAP5 to this test[47] is a good example of integral system behavior prediction capability and also provides an example of the benefits obtained by the use of an advanced hydrodynamic model. In particular, the RELAP5 results agree much better with data than the RELAP4 results. Test S-07-6 response was quite different from previous Semiscale experiments and was characterized by several periods in which refill of the downcomer and partial reflooding of the core was followed by a rapid reduction in both the downcomer and core liquid inventories (mass depletion).

*This test is one in a series of tests performed as a multinational project at the Marviken Power Station by A. B. Atomenergi Sweden. The test results are reported by L. Eriksson, et al., in "Interim Report Results from Test 4," MXC-204, May 1979.

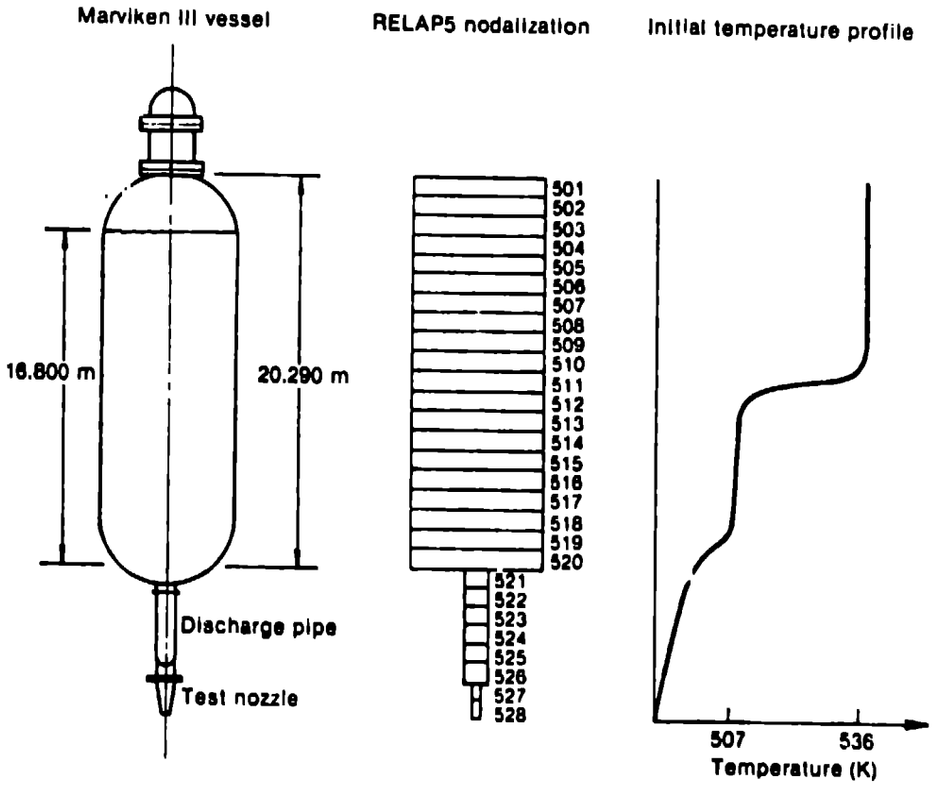

Fig. 8. Marviken III Test 4 vessel schematic, RELAP5 nodalization, and initial temperature profile.

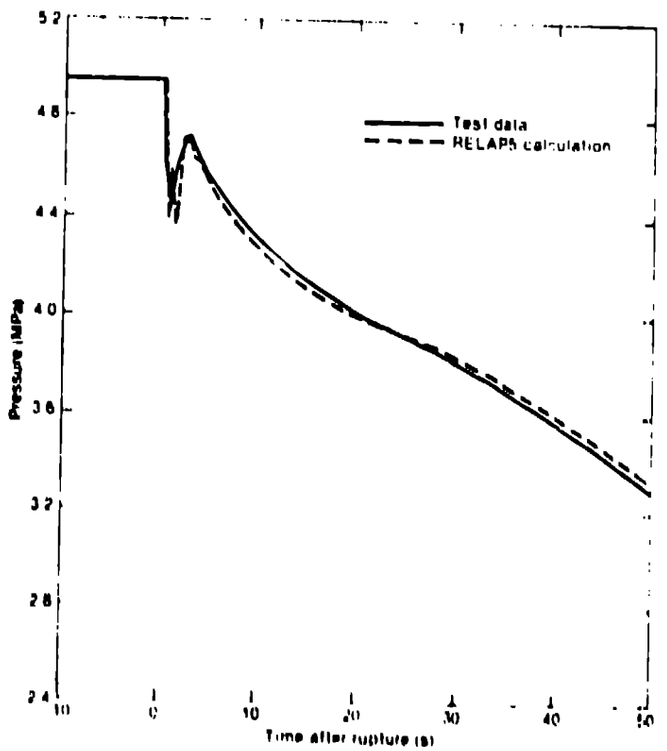

Fig. 9. Calculated and measured pressure at vessel top (Cell 501 in RELAP5 nodalization).

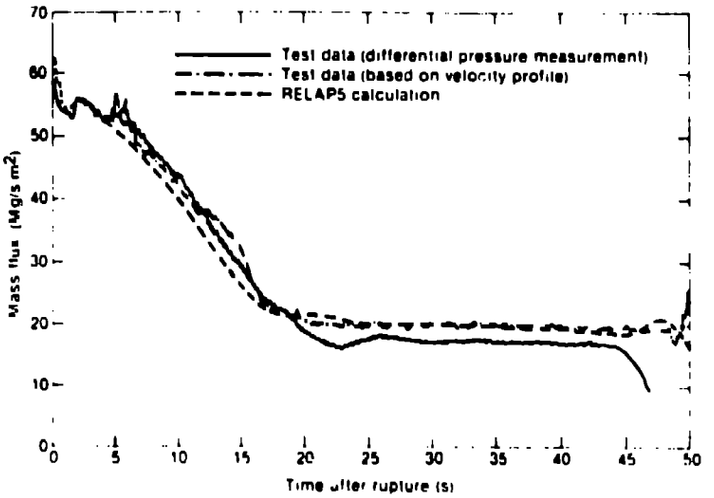

Fig. 10. Calculated and measured mass flux at nozzle inlet (Cell 526 in RELAP5 nodalization).

The flow oscillations resulted in core temperature oscillations, and complete quenching of the core did not occur until 500 s after rupture.

The RELAP5 model of the Semiscale Mod-3 system is divided into control volumes connected by junctions. The code uses component-oriented modeling so that large sections of the system can be identified as a component. The component can then be subdivided to obtain the needed detail. A schematic of the model for the Semiscale Mod-3 system is shown in Fig. 11. This nodalization diagram can be compared to the isometric drawing of the Semiscale system shown in Fig. 2. A total of 133 control volumes interconnected by 143 flow junctions were used. A total of 109 conduction heat structures (shown as shaded areas in Fig. 11) were used to represent heat transfer from piper and structural parts of the system. Twelve heat structures (one for each power step) were used to represent low-power heater rods.

The model was initialized by running the calculation at prescribed initial conditions until steady state was reached. The transient calculation was then made from the initiation of rupture through blowdown and reflood to 200 s. The core power, pump coastdown, and ECC rates were taken from the experimental data.

The break flow rate controls the rate at which the system empties, the depressurization rate, and the core flow behavior. The transition of break flow to two-phase flow was calculated to occur at 2 s, while the test data indicated two-phase choked flow at 1 s. The calculated break flow rate in the two-phase flow region was slightly higher than the measured data indicated. The slightly higher calculated total break flow rate resulted in slightly more rapid depressurization of the system. Figure 12 shows the calculated pressure at the vessel upper plenum. The calculated pressure was higher than shown by the test data before 5 s and lower thereafter.

In spite of slight discrepancies, the RELAP5 calculation of the blowdown behavior of the Mod-3 system was very good. This was reflected in the core heater temperature. Figure 13 shows the rod temperature in the hot channel at 184 cm above the bottom of the rod. The calculated temperature was taken at

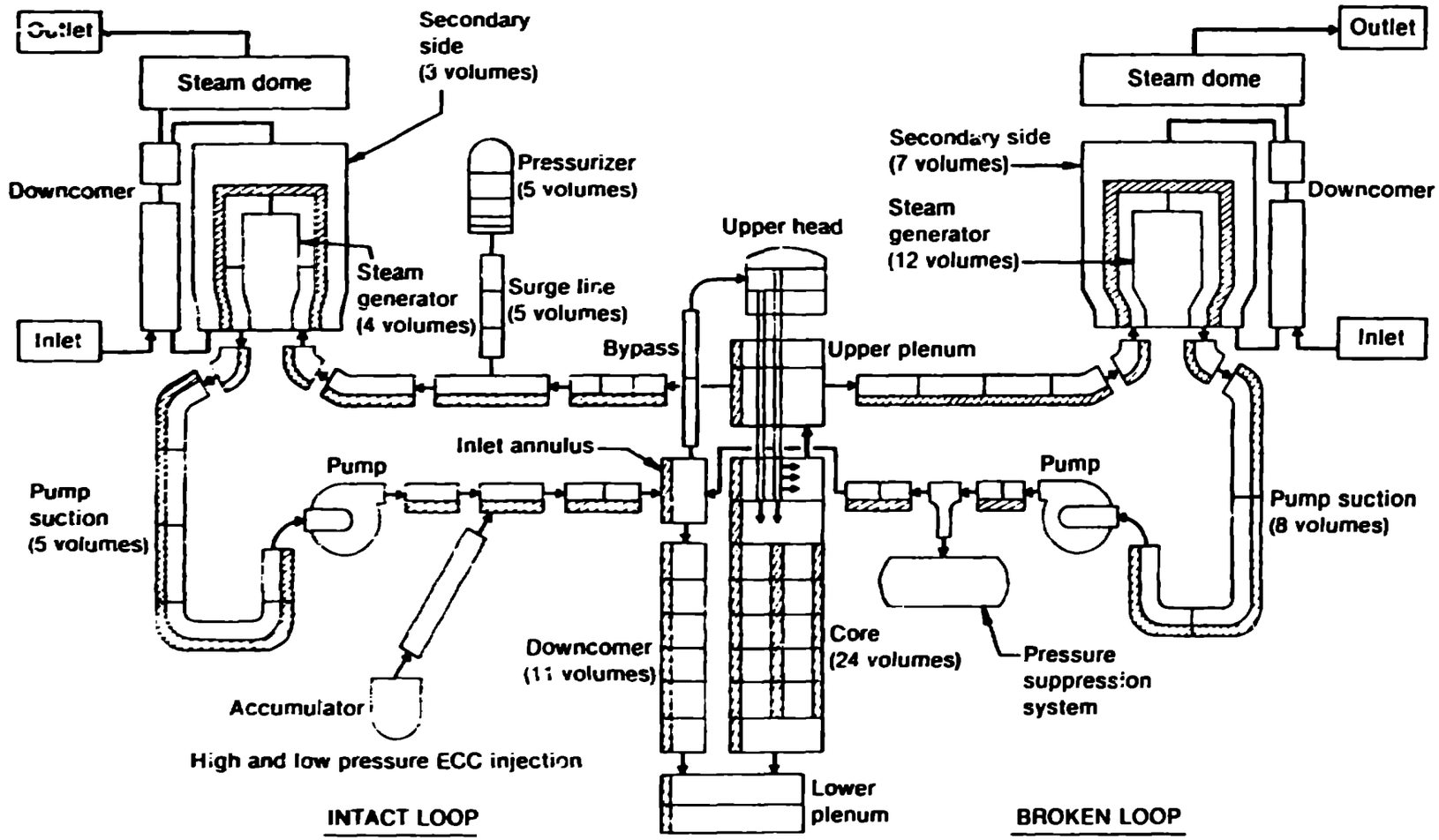

Fig. 11. RELAP5 [illegible] for Semiscale Mod-3 system.

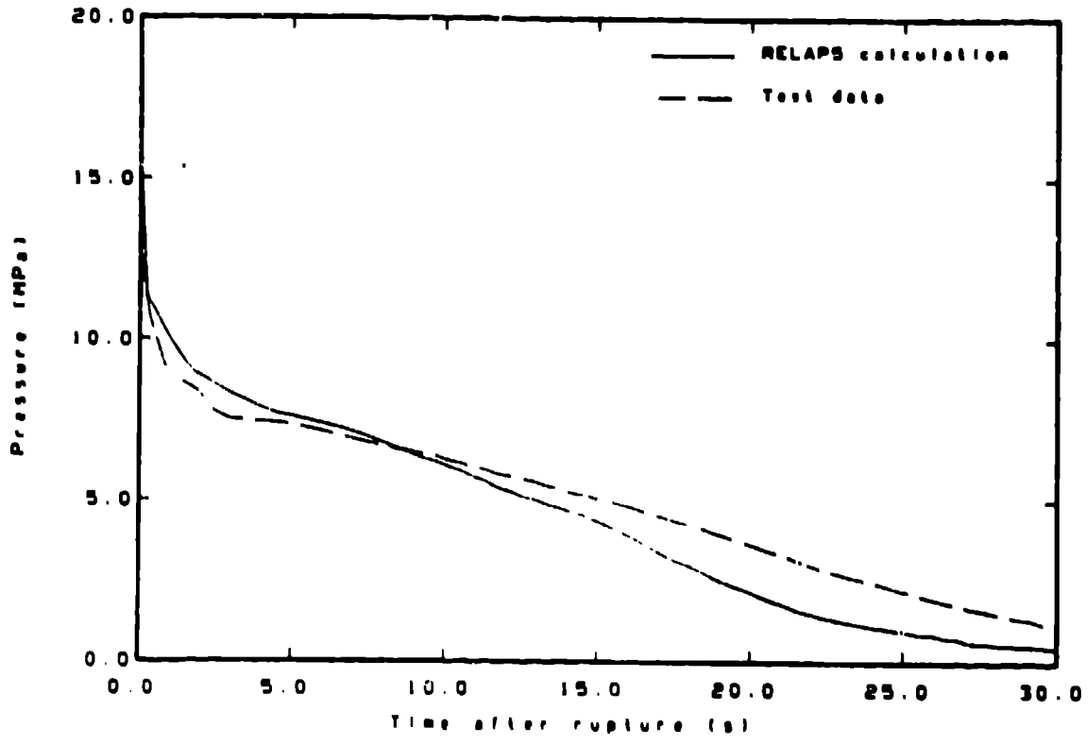

Fig. 12. Calculated and measured pressure in the upper region.

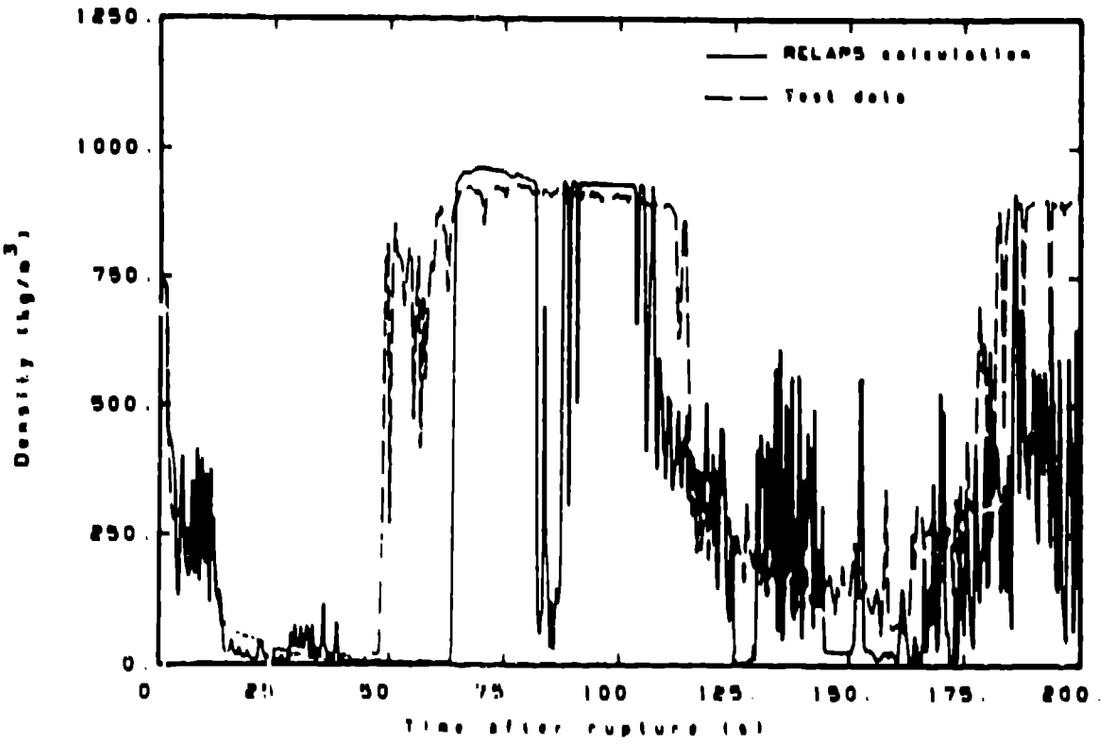

Fig. 13. Calculated and measured fluid density at the middle of downcomer.

slightly under the surface (80-K difference existed at the initial steady-state conditions). Calculated temperatures reached a peak of 1150 K, which agreed with the test data. The decrease in heater rod temperature beginning at about 12 s after rupture was a result of water draining from the upper head into the core.

The RELAP5 simulation of the phenomena associated with ECC injection, refill, and reflood were equally encouraging. The test was simulated from initiation of pipe rupture through reflood in one calculation without renodalization. At 19 s, the system pressure reached 4.14 MPa, and the ECC water from the accumulator began to flow into the system. During the accumulator ECC injection period, the difference in the calculated vapor and liquid temperature clearly indicated thermal nonequilibrium existed.

One of the most interesting aspects of Test S-07-6 was the multiple filling and emptying of the downcomer and core as mentioned earlier. The downcomer depletion behavior and the effect on the core thermal response during reflood was reflected in the fluid density. Figure 13 shows calculated and measured densities at the center of the downcomer. Both the calculated values for the density and the periodic mass depletion behavior compared well with the measured data. In the calculation, the ECC water penetrated into the downcomer at 65 s, while the test data showed this to occur at 50 s.

The oscillations in the downcomer mass flow were controlled by the time period when the subcooled water was present in the downcomer. When the fluid temperature reached the saturation temperature, vapor was generated and the hydrostatic head in the downcomer decreased. Some of the coolant was then expelled from the top of the downcomer. When the downcomer hydrostatic head decreased sufficiently as a result of mass depletion, the ECC water could again flow into the downcomer. The heating, expelling, and refilling process was repeated periodically.

The measured heater rod surface temperature rose and decreased as water left and entered the core. The calculation also showed the oscillation in the heater rod temperature. Figure 14 shows the calculated and measured rod temperatures at the hot and average channels near the axial peak power zone. The calculated maximum and minimum temperatures compared well with the test data before 100 s. The calculated frequency of the temperature oscillation was close to the measured frequency after 100 s. The calculated temperature of the hot channel gave a lower value while the temperature of the average channel was too high. The average of the two temperatures fell within the measured data. Two channels were used to model the core and no cross-flow was allowed between the two channels. This core model appears to be the cause for the discrepancy between the calculated and measured rod temperatures.

This analysis confirmed that Semiscale Mod-3 Test S-07-6 was modeled well by RELAP5 during the blowdown period and that it gives reasonable quantitative results for the refill and reflood periods of the test.

LOFT TEST L3-2. The results presented here represent the first time that the RELAP5 code was used for a formal pretest prediction.

A LOFT facility description and a summary of the LOCE L3-2 key events are included in Ref. 46. The nodalization used in the RELAP5 calculation was similar to the nodalization used for the RELAP4 blowdown calculation of LOFT LOCE L2-3.[48] In areas where significant elevation differences exist, the RELAP5 nodalization was increased to define steep density gradients. The

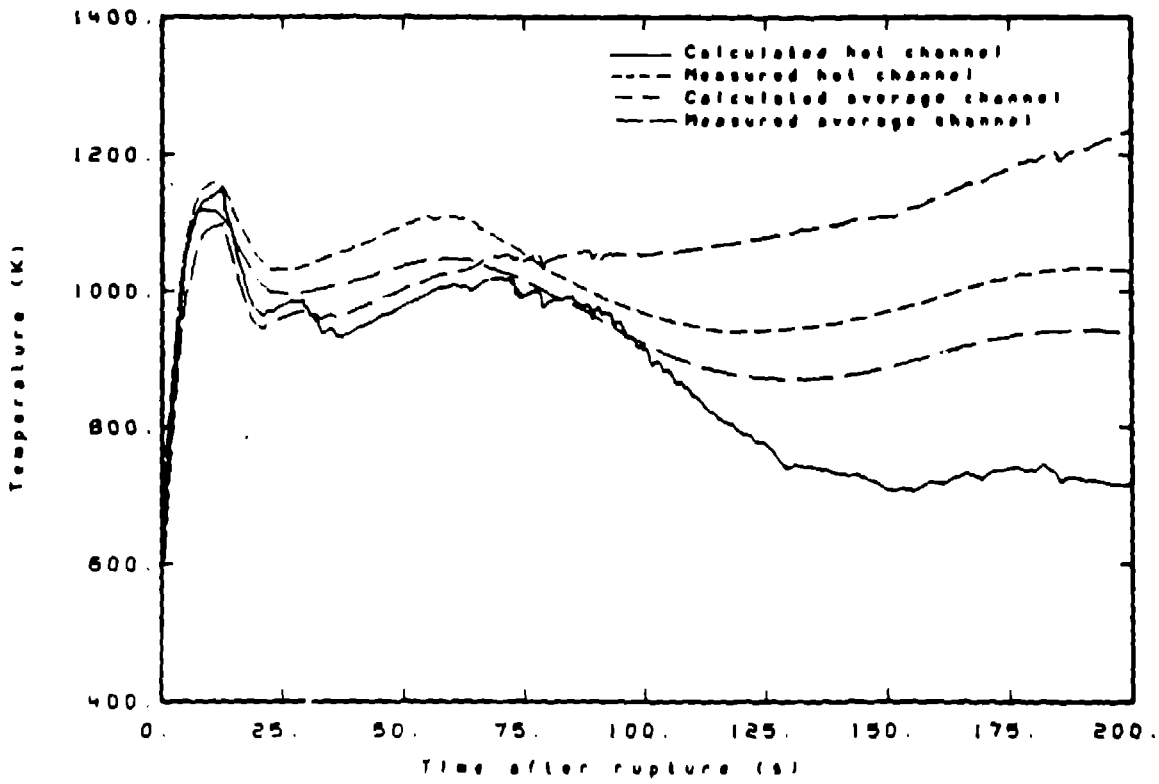

Fig. 14. Calculated and measured temperature of heater rod at the hot and averaged channels near axial power peak.

RELAP5 nodalization also includes simulation of the potential bypass flow path between the reactor vessel inlet annulus and upper plenum. The nodalization scheme is shown in Fig. 15.

The liquid separator and mist extractor of the steam generator secondary system are modeled by modifying the donor formulation of the convective terms at the separator junction (Component 10). The steam flow control valve is assumed to have a linear area change with stem position and a zero-inertia constant speed driver. The RELAP5/MOD0 valve subroutine required modification to model this type of valve. The sophisticated trip logic in RELAP5 allows simulation of the valve controller. The steam generator outflow is connected to the air-cooled condenser (Component 16) where the pressure is specified. The feed flow is input as a function of time.

The ECCS System is represented by Components 168, 500, and 505 (see Fig. 15). LOFT Accumulator A, Component 168, is modeled using the RELAP5 accumulator model. The LPIS and HPIS pump models, Components 505 and 500, respectively, required modification to the time-dependent junction subroutine in RELAP5 so that the flow provided by these components could be specified as a function of downstream pressure. The orifice at the break plane is modeled by a valve having an open area equal to the area of the drilled break orifice.

Heat conduction between the primary and secondary sides of the steam generator is through heat Structure 5-2, the steam generator tubes. The reactor pressure vessel, filler blocks, core filler, upper and lower core support structures, and core also were modeled using heat conductors. The system was modeled with no heat loss to the surroundings.

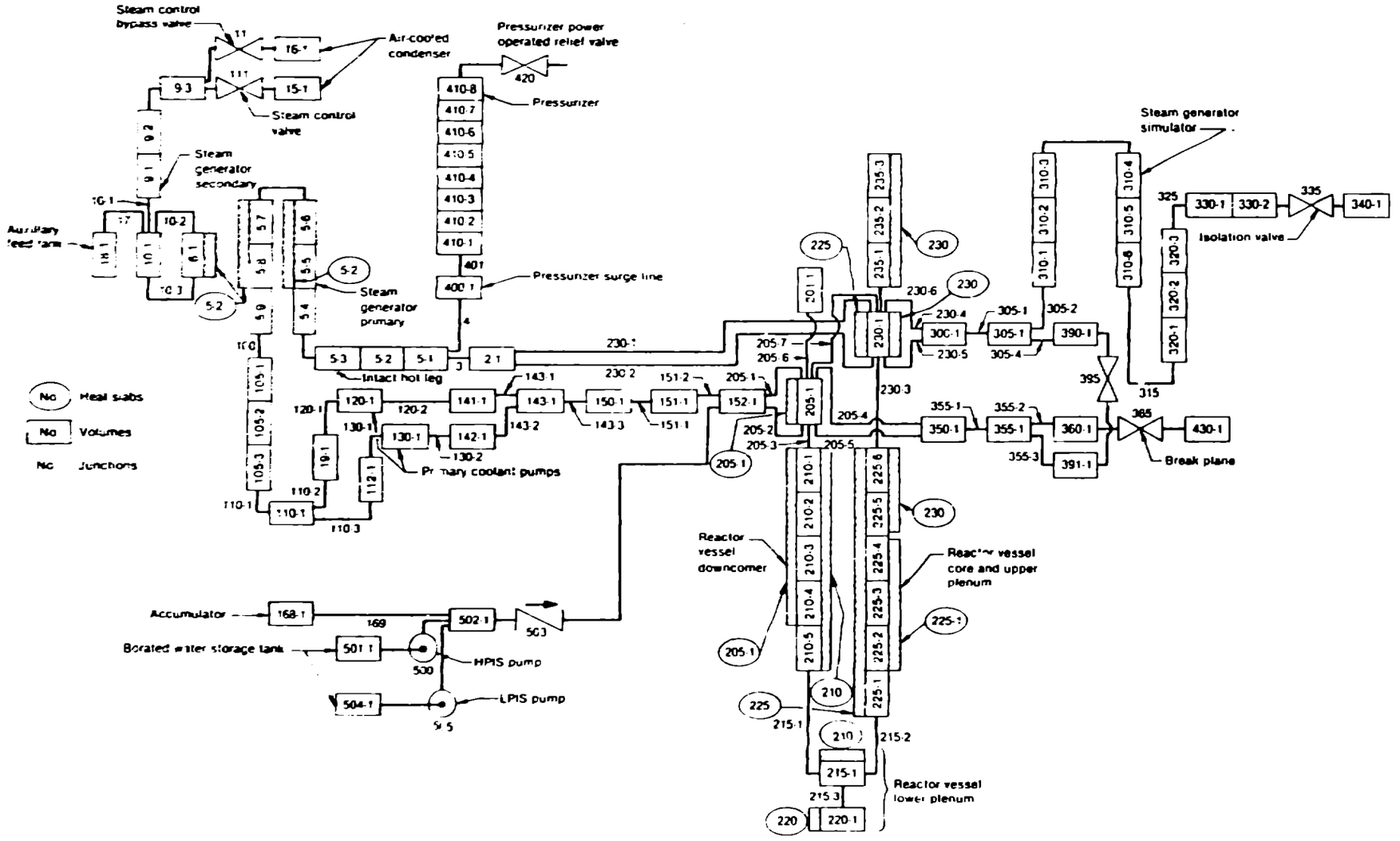

Fig. 15. LOFT RELAP5 model schematic diagram.

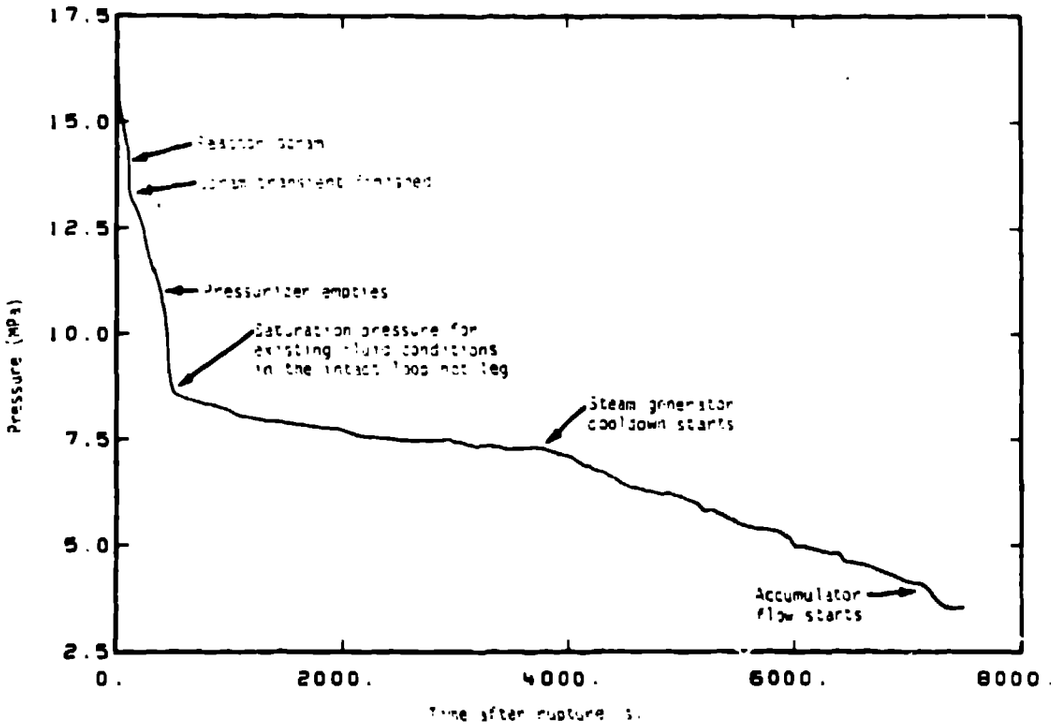

Fig. 16. RELAP5 predicted upper plenum pressure response.

The transient was initiated by opening the cold leg quick-opening blowdown valve. For the first 94 s after experiment initiation, the pressure is predicted to decrease 1.41 MPa from the initial value, causing a reactor scram to initiate as shown in Fig. 16. During the next 13 s, the steam generator removes more energy from the primary system than the reactor core adds, resulting in a net stored energy loss in the primary loop. The resulting density increase in the primary coolant places a further demand on the pressurizer, resulting in the high depressurization rate after 94 s. At 107 s, the steam flow control valve shuts completely, mitigating the rapid pressure decline in the primary system. At 127 s, HPIS is initiated by low pressure in the hot leg; but at about 400 s, the pressurizer empties and the primary system rapidly approaches the saturation pressure corresponding to the fluid temperature in the intact loop hot leg. The steam flow control valve is predicted to start opening at about 150 s. A small flow in the intact loop carries thermal waves, generated by the valve opening, throughout the system. The steam valve is predicted to stay closed in the period between 1000 and 2000 s and to start opening again at about 2000 s, reducing pressure to about 7.2 MPa. At this point, HPIS flow is about equal to break flow.

After 1 h, steam is removed from the steam generator by opening the steam flow control bypass valve in such a manner to cause cooling in the steam generator secondary side of 44.4 K per hour. This energy removal causes cooling in the primary loop of 42.5 K per hour. The calculations, therefore, indicate that the steam generator cooling will be effective in the primary system. After 1.1 h of cooldown, the auxiliary feed pump is turned on to fill the steam generator secondary side. The addition of this cold water causes a cooling rate in the steam generator greater than 44.4 K per hour. The steam flow control bypass valve is, therefore, shut whenever the cooldown exceeds 44.4 K per hour. The liquid level in the reactor vessel upper plenum was not

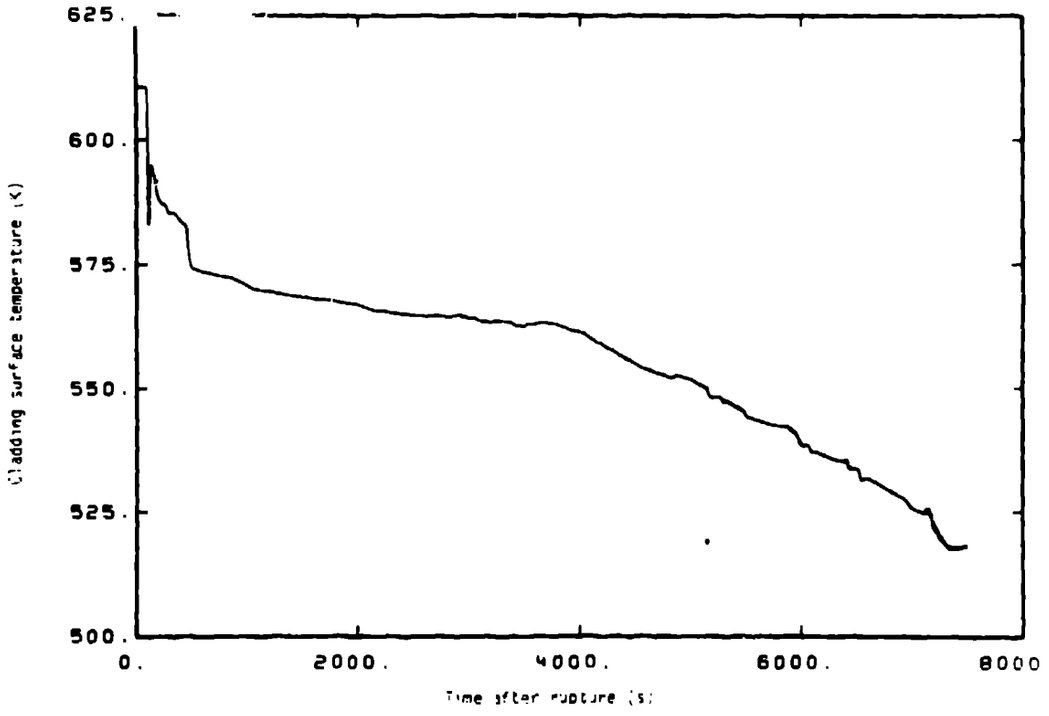

Fig. 17. RELAP5 predicted cladding surface temperature.

predicted to drop below the top of the active core, thus the cladding surface temperature response shown in Fig. 17 is calculated to be benign.

The calculations shown here were run faster than the simulated time, i.e., less than 7500 s of CDC-7600 CPU seconds were required to simulate system behavior to 7500 s. The faster-than-real time calculational speed achieved in this application was a milestone in the RELAP5 code development. The achievement of real time computational capability suggests the possibility of future applications such as system simulators, on-line diagnostic computation, and system control.

5. TRAC DESCRIPTION AND EXAMPLE COMPUTATIONS

This section presents a summary overview of the Transient Reactor Analysis Code (TRAC) and a few comparisons between TRAC calculations and experimental data. Detailed descriptions of TRAC are given in Refs. 8 and 49, while a summary of several experimental comparisons is given in Ref. 50.

5.1 Goals and Development Guidelines

A key goal of the TRAC development effort is to provide an advanced best-estimate LWR systems code that can credibly predict the accident behavior of LWRs. The desired predictive credibility is to be established through the careful assessment of code calculations against a sufficiently broad range of pertinent experimental data.

To accomplish this goal, the following guidelines for the development of the initial versions of TRAC were adopted.

1. Eliminate user-selected modeling options and parameter variations (or "tuning dials") to the degree possible. If numerous combinations of modeling options are used in assessing a code against various experiments, it is difficult to know what options might be appropriate for a new situation where no direct experimental data exist (e.g., an accident in an actual reactor). The goal of the TRAC assessment effort is to predict adequately a broad range of experiments with no user tuning from one test to the next.

2. Model important physical phenomena in as fundamental a way as is practical. Basic modeling should generally extrapolate to new situations with more reliability than highly empirical approaches. Such basic modeling also tends to provide more detail on the thermal-hydraulic behavior of a system.

3. Provide sufficient flexibility to allow modeling of all major LWR designs and pertinent experimental configurations.

Versions of TRAC developed according to the above guidelines are referred to as "detailed" versions.

An additional goal of the TRAC effort is to provide fast running code versions that can be used for such applications as parametric studies, scoping calculations, licensing applications, and very long transients (e.g., small breaks). Some of the major guidelines being followed in the development of the fast running versions are as follows.

1. Use less detailed (and usually more empirical) modeling to achieve short running times.

2. Keep as much in common as possible between the fast running and detailed versions to minimize the amount of needed experimental assessment.

3. Calibrate the fast running versions against the carefully assessed detailed versions for specific applications.

5.2 Development Status

The initial versions of TRAC were detailed versions designed primarily to analyze large-break LOCAs in PWRs. The first version, TRAC-P1, was released by The Los Alamos Scientific Laboratory (LASL) on a limited basis in March 1978. An improved version, TRAC-P1A,[8] was released through the National Energy Software Center in March 1979. A further refined and improved version, called TRAC-PD2,* is scheduled for release in the spring of 1980.

The initial fast running version, TRAC-PF1, is currently under development at LASL. The experimental assessment process will start in the spring of 1980, with its public release planned for late 1980. The development of BWR

*All future versions of TRAC will be designated as TRAC-xyz, where x=P for PWR versions and = B for BWR versions; y=D for detailed versions and = F for fast running versions; and z is a version identification number.

versions is being carried out at the Idaho National Engineering Laboratory (INEL). The initial BWR version, TRAC-BD0, was completed in February 1980. The first BWR release version, TRAC-BD1, is under development.

TRAC-P1A will be used as a reference version for this paper. In some cases, the modeling in TRAC-PD2 (as well as calculated results) will be referred to, however.

5.3 Model Description

Some of the important modeling characteristics of TRAC-P1A are summarized in the following section. These characteristics typically reflect the state of the art in the various areas and were incorporated in pursuit of the goals and guidelines outlined above for detailed versions of TRAC.

Multidimensional Fluid Dynamics. Although the flow within the ex-vessel components is treated in one dimension, a full 3-D (r,θ,z) flow calculation can be used within the reactor vessel. This is done to allow an accurate calculation of the complex multidimensional flow patterns inside the reactor vessel that can play an important role in determining accident behavior. For example, phenomena such as ECC downcomer penetration during blowdown, multidimensional plenum and core flow effects, and upper plenum de-entrainment and fallback during reflood can be treated directly.

The flow can be blocked across specified boundaries within a vessel to allow modeling of internal structures such as the downcomer. Flow restrictions can also be specified as appropriate to model structures like core support plates. One-dimensional components can be connected to any vessel mesh cell face (including interior mesh cells) to model the appropriate loop connections. Each of these features is illustrated in Fig. 18 where a simplified 3-D vessel noding is illustrated.

The 3-D hydrodynamics treatment in the vessel will reduce to 2-D (x-y) or even 1-D geometry when this is appropriate.

Nonhomogeneous, Nonequilibrium Modeling. A full two-fluid (six-equation) hydrodynamics approach is used to describe the steam-water flow within the reactor vessel, thereby allowing such important phenomena as countercurrent flow to be treated explicitly. The flow in the 1-D loop components is described using a five-equation drift-flux model, which differs from the standard four-equation drift-flux approach by the addition of a separate vapor energy equation. Thus, it is not necessary to make any assumptions regarding the temperature of either phase. This provides a consistent nonequilibrium thermodynamic treatment in both the vessel and loop components and permits more accurate modeling of the fluid dynamics through a direct treatment of flashing and condensation effects.

Flow-Regime-Dependent Constitutive Equation Package. The basic field equations must be supplemented by a number of so-called constitutive equations to obtain closure. These equations describe the transfer of mass, momentum, and energy between the steam-water phases as well as the interaction of these phases with the system structure. Because the nature of these interactions is strongly dependent on the flow topology, a flow-regime-dependent constitutive equation package has been incorporated into the code. The ability of TRAC to successfully meet its goal of eliminating user-selected modeling options

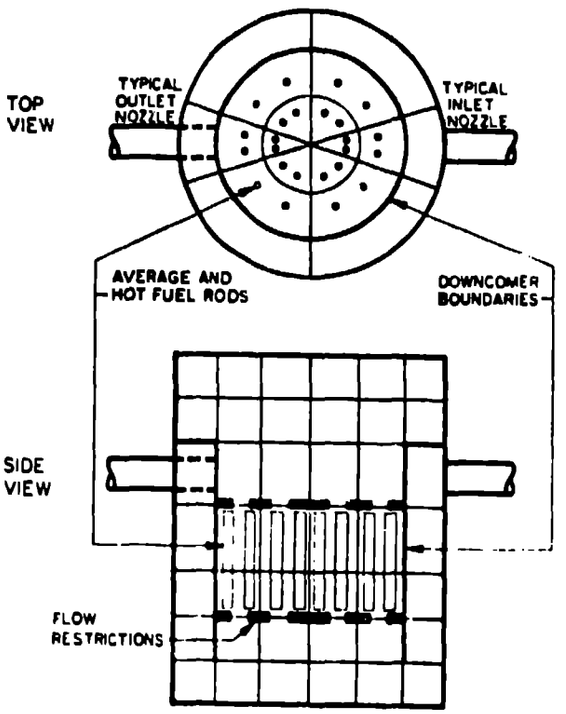

Fig. 18. Illustration of TRAC 3-D configuration.

hinges on the ability of this package to recognize flow regimes adequately and to supply appropriate correlations. The flow regimes currently considered are bubbly, slug, and annular (or annular mist) with appropriate transition regions.

In the case of the five-equation drift-flux model used in 1-D components, the interphase slip correlation is also flow-regime dependent. A flow-regime map has also been incorporated into TRAC for this purpose. This is shown in Fig. 19 to serve as an illustration of the form of these maps. As can be seen, the flow-regime selection is made on the basis of void (steam) fraction and the magnitude of the overall mass flux.

The details of the constitutive equation package are beyond the scope of this chapter; however, many of the phenomena and correlations are discussed in other chapters. The specific correlations used in TRAC-P1A are given in Ref. 8. Although the constitutive relations in TRAC will be improved in the future, assessment calculations performed to date indicate that a fairly wide range of conditions can be adequately treated with the current package.

Comprehensive Heat Transfer. Heat transfer models in TRAC include conduction models to calculate temperature fields in structural materials and fuel rods, and convection models to provide heat transfer between structure and coolant. Heat transfer to the two-phase fluid is calculated using a generalized boiling curve constructed from a library of heat transfer correlations based on local surface and fluid conditions. The heat transfer regimes and correlations used for this purpose[8] are summarized in Table IV.

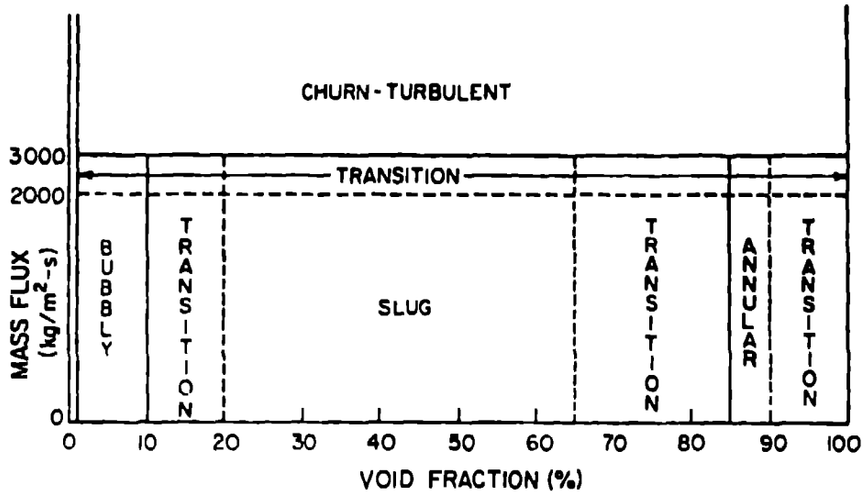

Fig. 19. TRAC flow regime map for slip correlations.

TABLE IV

HEAT TRANSFER CORRELATIONS IN TRAC-P1A

Regime	Correlation
Forced convection to single-phase liquid	laminar flow : constant Nusselt number turbulent flow : Dittus-Boelter
Nucleate boiling and forced convection vaporization	Chen
Critical heat flux	low flow : Zuber pool boiling high flow : Biasi
Transition boiling	log-log interpolation
Minimum stable film boiling	low pressure : Henry-Berenson high pressure : homogeneous nucleation
Film boiling	modified Bromley Dougall-Rohsenow
Forced convection to single-phase vapor	free convection : McAdams turbulent flow : Dittus-Boelter
Forced convection to two-phase mixture	laminar flow : constant Nusselt number turbulent flow : Dittus-Boelter
Horizontal film condensation	Chato
Vertical film condensation	Nusselt theory
Turbulent film condensation	Carpenter and Colburn

Conduction models are used to calculate temperature fields in 1-D (cylindrical) pipe walls, lumped-parameter slabs, and 1-D (cylindrical) fuel rod geometries. Pipe wall conduction is used in the components outside the vessel, whereas the slab and fuel rod conduction models are used in the vessel module. The fuel rod conduction analysis accounts for gap conductivity changes, metal-water reaction, and quenching phenomena. A fine-mesh axial renoding capability is available for fuel rods to allow more detailed modeling of reflood heat transfer and tracking of quench fronts due to bottom flooding and falling films.

In TRAC-P1A, quench fronts are advanced using an empirical velocity correlation. Experience with this approach has indicated that it is difficult to model low flooding rate experimental data accurately. A new reflood model has been incorporated into TRAC-PD2 that explicitly accounts for axial heat conduction near the front.

Each fluid mesh cell in the core region can contain an arbitrary number of fuel rods for the purpose of fluid dynamics calculations. However, heat transfer calculations are only performed on one average rod and one hot rod in each core mesh cell as shown in Fig. 18. The average rod represents the average of the ensemble of rods in the mesh cell, and its thermal calculation couples directly to the fluid dynamics. A spatial power peaking factor and local fluid conditions in the mesh cell are used in the hot rod calculation, but this calculation does not feed back to the hydrodynamics. The total core power level is determined from either a table lookup or from the solution of the point-reactor kinetics equations, including decay heat (6 delayed neutron groups and 11 decay heat groups). The spatial power distribution is specified by separate radial and axial power shapes in the core plus a radial distribution in the fuel rod.

Component and Functional Modularity. TRAC is completely modular by component. The component modules are assembled through input data to model virtually any PWR design or experimental configuration. This gives TRAC great versatility in the possible range of applications. It also allows component modules to be improved, modified, or added without disturbing the remainder of the code. Modules are available to model accumulators, pipes, pressurizers, pumps, steam generators, tees, valves, and vessels with associated internals.

TRAC is also modular by function. This means that the major aspects of the calculations are performed in separate modules. For example, the basic 1-D hydrodynamics solution algorithm, the wall temperature field solution algorithm, heat transfer coefficient selection, and other functions are performed in separate sets of routines that are accessed by all component modules. This type of modularity allows the code to be readily upgraded as improved correlations and experimental information become available.

5.4 Numerical Methods

A summary of the basic numerical methods in TRAC is given in this section. A more detailed description of the finite difference equations and solution strategy is presented in Appendix A.

The system of field and constitutive equations is solved using a staggered differencing scheme[51,52] on an Eulerian mesh. In this approach, the velocities are located at the mesh cell surfaces, while volume properties such as pressure, temperature, energy, and density are located at the mesh cell centers. A semi-implicit time differencing is normally used, with donor

cell averaging employed to produce stability. When the semi-implicit approach is used, a standard Courant stability criterion must be observed.

The 1-D flow equations are written in two separate finite difference forms. One form is the semi-implicit, staggered difference approach mentioned above.[53] The second form is an unconditionally stable fully implicit approach.[54] The latter form is used in 1-D components where very high flow velocities are expected locally (such as near a break during the blowdown phase of a LOCA). In such cases, the fluid velocity Courant condition would necessitate very small time-step sizes in a semi-implicit formulation. A fully-implicit component can then be substituted. Thus, TRAC allows the user to blend semi- and fully-implicit formulations in the same calculation to improve computing efficiency. The actual finite-difference equations used in TRAC are too lengthy to reproduce here (especially the 3-D equations). The 1-D drift-flux equations are given in Appendix A, while the others can be found in Ref. 8.

Iterative methods are generally used to solve the finite-difference equations. Each time step in the transient calculation consists of several passes through all the components in the system. These passes, whose purpose is to converge to the solution of the nonlinear finite-difference equations, are called outer iterations. If the outer iteration process fails to converge, the integration time step size is reduced and the time step is repeated.

The solution procedure during an outer iteration begins with a linearization of the equations for each 1-D component. This results in a block tridiagonal system in which linear variations in pressure and other independent variables (vapor fraction, liquid temperature, and vapor temperature) are solved in terms of variation in the junction velocities for the component. If there are no vessels in the calculation, these linearized equations are combined with the linearized junction momentum equations to obtain a closed linear system for the junction velocity variations. This system is solved by direct methods and a back substitution is made to update the remaining independent variables. Therefore, there is no inner iteration process involved for 1-D components.

When one or more vessels are present, the variations in the 1-D component junction velocities are solved in terms of the pressure variations at the vessel junctions. These equations are combined with the remaining linearized equations in the vessel to provide a closed set of linear equations. Because the matrix is usually too large for direct inversion, this set of linear equations is solved by Gauss-Seidel iteration (an option that allows for a direct inversion in the case of relatively small problems has recently been made available). When this vessel inner iteration process has converged, back substitution through the 1-D components again completes the solution of the full linear system. A single pass through this procedure provides the solution for the linearized finite difference equations. Subsequent passes for the same time step result in a Newton-Raphson iteration scheme with quadratic convergence on the nonlinear difference equations.

A steady-state capability is also included in TRAC to provide time-independent solutions. These may be of interest in their own right or can serve as initial conditions for subsequent transient calculations. Two types of calculations are available within the steady-state capability: (1) a Generalized steady-state calculation and (2) a PWR initialization calculation.

The first is used to find steady-state conditions for a system of arbitrary configuration. The second is applicable to PWR systems and is used to adjust certain loop parameters to match a set of user-specified flow conditions.

Both calculations utilize the transient fluid dynamics and heat transfer routines to search for steady-state conditions. The search is terminated when the normalized rates of change of fluid and thermal variables are reduced below a user-specified criterion throughout the system. For a given problem, computer running times for steady-state calculations are generally much smaller than those for transient calculations.

All TRAC versions to date have been developed on CDC-7600 computers. TRAC-PD2 is currently being converted for use on the CRAY-1. It is anticipated that future release versions will also be converted for use on IBM computers. Fast running versions will additionally be available for use on DEC/VAX machines. Computer running time is highly problem dependent. It is a function of the total mesh cells in the problem and the maximum allowable time step size. The total run time for a given transient can be estimated from a unit run of 2 to 3 ms per mesh cell per time step on a CDC-7600 with an average time step size of 5 ms.

5.5 TRAC Example Calculations

A major part of the TRAC development effort involves the comparison of calculations with experimental data. This experimental assessment process proceeds in two phases. The first phase, called developmental assessment, is an integral part of the code development effort. It consists of numerous posttest analyses of experiments covering all aspects of LOCA phenomenology and serves as an aid to model development and evaluation. A code version is not released until it has adequately analyzed a predetermined set of experiments. Data comparisons from nine experiments were formally documented as part of the release of TRAC-P1A.[50] These experiments are listed in Table V to illustrate the scope of the developmental assessment process. The assessment set to be documented with the release of TRAC-PD2 is considerably larger.

Following the release of a given version of TRAC, an independent assessment phase is initiated. This phase emphasizes blind pretest predictions to establish predictive capability. The independent assessment to date has emphasized LOFT experiments but is expanding to include other facilities such as LOBI and the Japanese Cylindrical Core Test Facility.

Detailed comparisons of TRAC calculations and experimental data have been published elsewhere; thus, only a brief summary of two test comparisons from Ref. 50, followed by a more recent LOFT comparison, will be presented here. The first is an analysis of some countercurrent flow experiments performed at Creare, Inc., to study ECC downcomer bypass phenomena. This serves to illustrate the use of separate-effects tests in the model development process. The other two will be analyses of a semiscale and a LOFT experiment to illustrate the role of systems data comparisons.

Creare Countercurrent Flow Experiments. The Creare countercurrent flow experiments investigated the effects on ECC penetration to the lower plenum of countercurrent steam flow rate, downcomer wall superheat, and ECC subcooling. The basic component of the Creare test facility is a 1/15-scale (linear dimension), multiloop, cylindrical model of a PWR downcomer region. A detailed description of this facility and its operation is given in Ref. 55. The configuration used in the tests analyzed here is the so-called "base-line"

TABLE IV

TRAC-P1A DEVELOPMENTAL ASSESSMENT ANALYSES

No.	Experiment	Thermal - Hydraulic Effects
1	Edwards Horizontal Pipe Blowdown (Standard Problem 1)	Separate effects, 1-D critical flow, phase change, slip, wall friction
2	CISE Upheated Pipe Blowdown (Test 4)	Same as 1 plus pipe wall heat transfer, flow area changes, and gravitational effects
3	CISE Heated Pipe Blowdown (Test R)	Same as 2 plus critical heat flux (CHF)
4	Marviken Full-Scale Vessel (Test 4)	Same as 1 plus full-scale effects
5	Semiscale 1-1/2 Loop Isothermal Blowdown (Test 1011, Standard Problem 2)	Synergistic and systems effects 1-D flow, phase change, slip wall friction, critical nozzle flow
6	Semiscale Mod-1 Heated Loop Blowdown (Test S-02-8, Standard Problem 5)	Same as 5 plus 3-D vessel model with rod heat transfer including nucleate boiling, DNB, and post-DNB
7	Creare Countercurrent Flow Experiments	Separate effects, countercurrent flow, interfacial drag and heat transfer, condensation
8	FLECHT Forced Flooding Tests	Separate effects, reflood heat transfer, quench front propagation, liquid entrainment and carryover
9	Nonnuclear LOFT Blowdown with Cold Leg Injection (Test L1-4, Standard Problem 7)	Integral effects during blowdown and refill, scale midway between Semi-scale and full-scale PWR

configuration having a 0.0127-m (0.5-in.) downcomer gap and a "deep plenum" geometry. The vessel has four cold legs oriented 90° to each other. Three of these legs are assumed to be "intact" and are connected to ECC injection lines. A single "broken" leg connects to the pressure suppression tank.

The test procedure is as follows. A constant steam flow rate through the vessel is established. The steam enters at the top of the vessel, flows down the center of the vessel into the lower plenum, up the downcomer, and out the broken cold leg. After reaching a steady steam flow rate, water is injected simultaneously into the three intact cold legs at a constant preset flow rate. After a short transient period, the plenum normally begins to fill. The test is run until the lower plenum is full or until the filling rate can be determined. A complete penetration, or flooding, curve is composed of a set of tests at a given liquid injection rate and liquid temperature with the steam flow rate varied over a range such that water delivery ranges from complete delivery to complete bypass.

The TRAC model of the Creare vessel is shown in Fig. 20. The 3-D vessel module used 112 computational cells with the mesh lines indicated in the figure.

The calculational procedure paralleled the Creare experimental procedure. A steady-state calculation was performed to establish a constant reverse steam flow and lower plenum pressure. This steady-state calculation was run until J^*_{gc} (the dimensionless reverse core steam flow rate) reached a constant value. This normally took about 3 s of simulation time. The transient calculation was then started with the initiation of ECC injection into the three intact cold legs. Results for two ECC injection rates and levels of subcooling are compared in Fig. 21. The low subcooling cases injected 30 gpm of ECC water at 212°F, while the high subcooling cases injected 60 gpm at 150°F. The reactor scale injection flow rate is 60 gpm. The system pressure ranged from 1 to 3 atm.

The basis for selecting these two penetration curves was to separate the basic phenomena determining whether ECC bypass or delivery will occur. These phenomena are interfacial momentum and energy exchange between the liquid and the steam. For a low subcooling case, the only effect that can produce bypass is the interfacial drag between the steam and the liquid. The calculated penetration curve for this case gives an appraisal of the constitutive relationship describing interfacial momentum exchange. Moreover since the calculations cover the range of complete bypass to complete dumping, different flow regimes exist in the downcomer at the bypass point than at the complete delivery point. In the high subcooling case, the interfacial heat transfer becomes significant in determining the quantity of liquid delivered. As can be seen, the TRAC calculations agreed very well with both of the experimental penetration curves. Comparisons such as these indicate that complex multidimensional phenomena, such as ECC bypass, can indeed be modeled with the rather fundamental modeling approach taken in the detailed versions of TRAC.

Semiscale Test S-02-8. Test S-02-8 was a simulation of a PWR double-ended cold-leg break performed in the semiscale Mod-1 facility.[56] In the Mod-1 configuration, nuclear heating is simulated with 40 electrically heated rods. The TRAC model of this experiment is shown in Fig. 22. This figure illustrates how the various TRAC components are connected to simulate a PWR type configuration. The calculation involved nearly every TRAC component module. The model had a total of 111 mesh cells in the 1-D loop components and 152 cells in the 3-D vessel component.

The initial steady-state conditions calculated with TRAC for use at the start of blowdown agreed very well with the experimental data. Some of the key transient results are compared in Figs. 23-25. The calculated and measured lower plenum pressures agree quite well as can be seen in Fig. 23. This indicates that TRAC did a reasonable job of analyzing overall system performance. A comparison of the cladding temperatures in the highest power region is shown in Fig. 24. The calculated results are compared with a band of measured values that encompassed all the cladding thermocouples in the lower half of the highest power step in Semiscale. With the exception of a slightly advanced departure from nucleate boiling, TRAC does an excellent job of predicting the cladding temperature response in this high power zone.

The final comparison presented is the hot-leg break mass flow rate shown in Fig. 25. The small rise in the flow rate at about 12 s is due to a slug of higher density fluid coming from the intact hot leg. The TRAC results show a small rise at this time, but underpredict the magnitude. In general, however, break flow rates were predicted quite well without the use of any empirical break flow model.

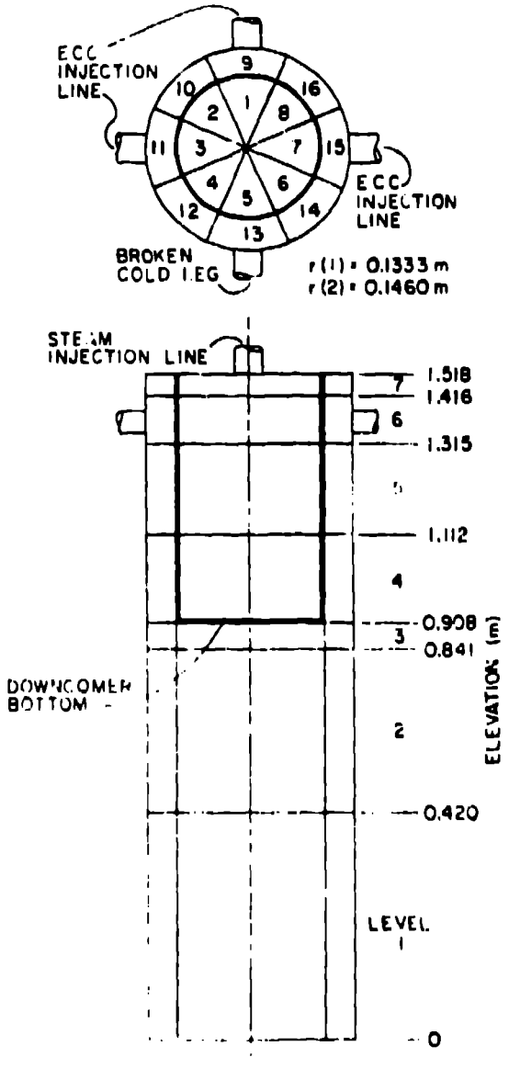

Fig. 20. TRAC noding for Creare 1/15-scale vessel.

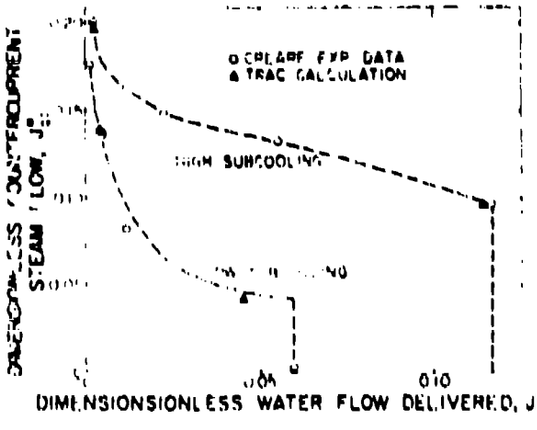

Fig. 21. Flooding curves for Creare experiments.

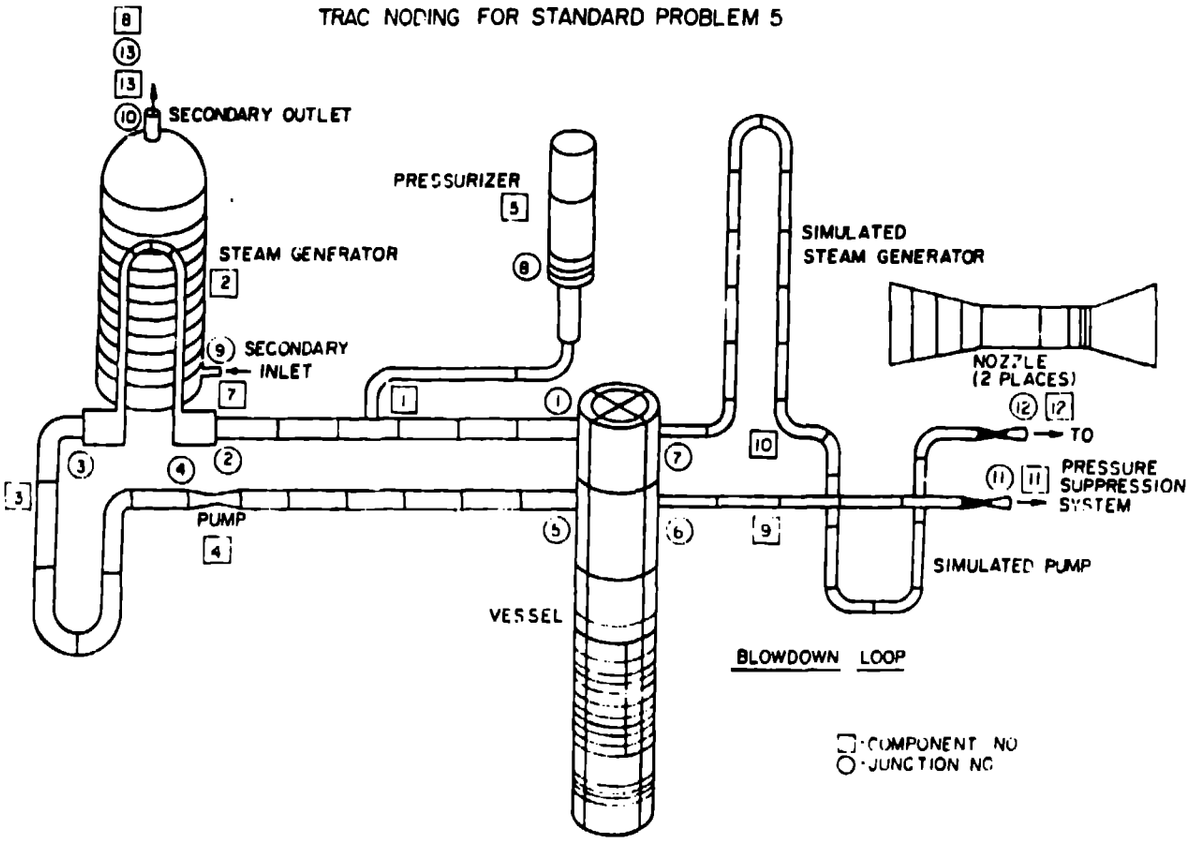

Fig. 22. TRAC noding and component schematic for Semiscale Mod-1 system.

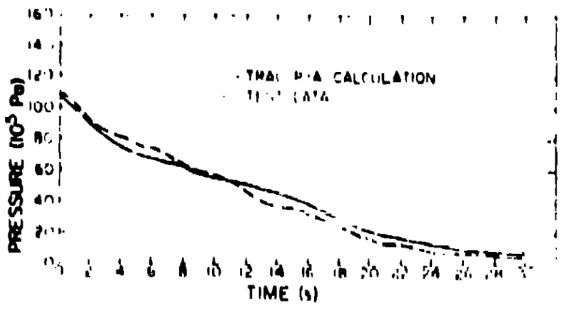

Fig. 23. Lower plenum pressure for Semiscale Test S-02-8.

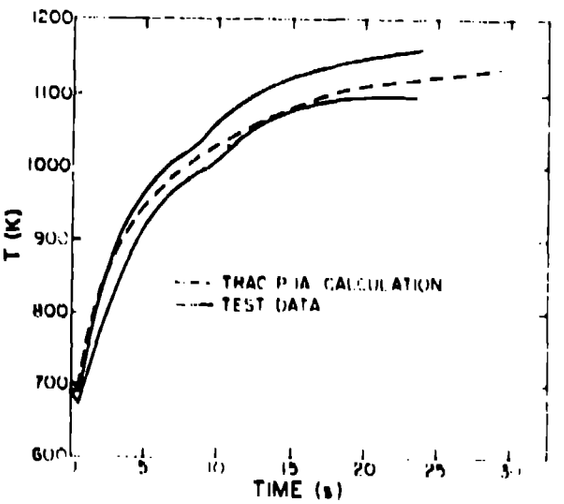

Fig. 24. Cladding temperature in high power zone for Semiscale Test S-02-8.

LOFT Test L2-3. Because LOFT is the only available nuclear-heated integral-effects test facility, several of the recent LOFT tests have been extensively analyzed with TRAC. This has included both blind pretest predictions and extensive posttest analyses. As an example, a few key results from Test L2-3 will be compared with the TRAC pretest predictions.

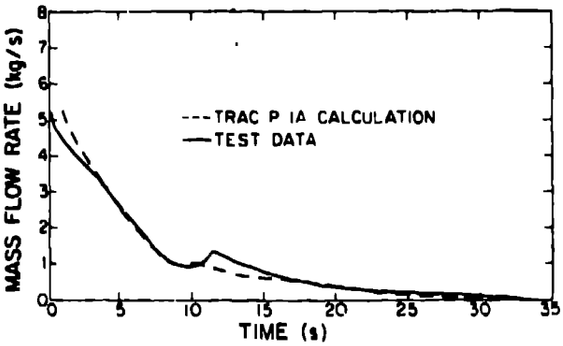

Fig. 25. Hot-leg break mass flow rate for Semiscale Test S-02-8.

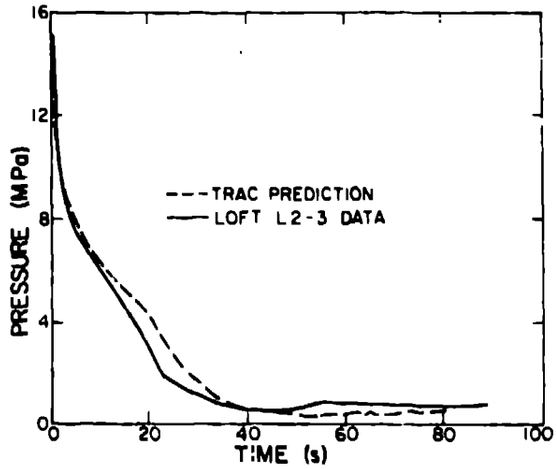

Fig. 26. Upper plenum pressure for LOFT Test L2-3.

Test L2-3 simulated a double-ended cold leg break and was conducted from an initial power of 37 Mwt.[57] The TRAC model consisted of 27 components with a total of 322 fluid mesh cells. There were a total of 12 axial levels in the vessel, including 5 axial levels within the core region. A total of 192 fluid cells were used within the vessel, including 60 within the core itself. The reflood fine mesh was initiated 10 s after accumulator injection started. There were 5 uniform fine-mesh intervals for each axial level, giving a total of 25 fine cells.

The initial system thermal and hydraulic conditions for the pretest calculation were obtained using the steady-state option. Good agreement was obtained between the calculated and measured conditions.

Pretest transient results are compared with the data[50] in Figs. 26-29. The upper plenum pressure is shown in Fig. 26. The calculation depressurized somewhat more slowly than the data and resulted in delayed ECC injection. Figure 27 shows the broken loop cold-leg mass flow rate. The early underprediction of the break flow is consistent with the overprediction of system pressure. In general, however, these results are in quite good agreement.

One of the more interesting (and unexpected) results from the early nuclear-heated blowdown tests in LOFT was the observed early rewet behavior in the high-power core region. The TRAC pretest predictions for an earlier test in this series (L2-2) had predicted rewet to occur in the lower power regions, but did not predict early rewetting in the high power region. It was suspected that the minimum film boiling correlation in TRAC-P1A might be at fault because it was based on low pressure data. The minimum film boiling correlation of Iloeje[59] was subsequently tried and found to give much better results. Because of this, two blind pretest predictions of Test L2-3 were performed. One used the standard release version of TRAC-P1A, while the second had the Iloeje correlation implemented. Temperatures from these two predictions are compared with data in Figs. 28 and 29.

The temperatures in a low-power peripheral region are compared in Fig. 29. As can be seen, both of the TRAC pretest predictions agreed quite well

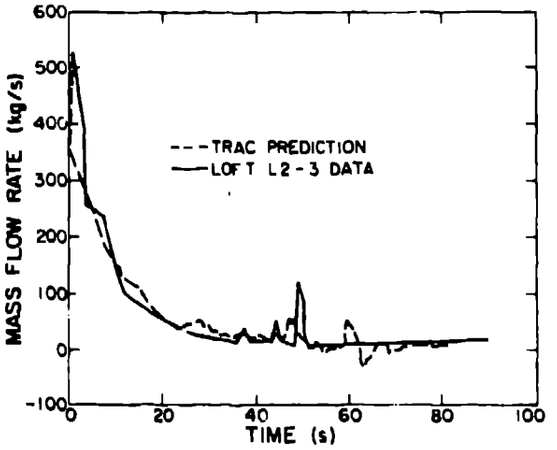

Fig. 27. Broken loop cold-leg mass flow rate for LOFT Test L2-3.

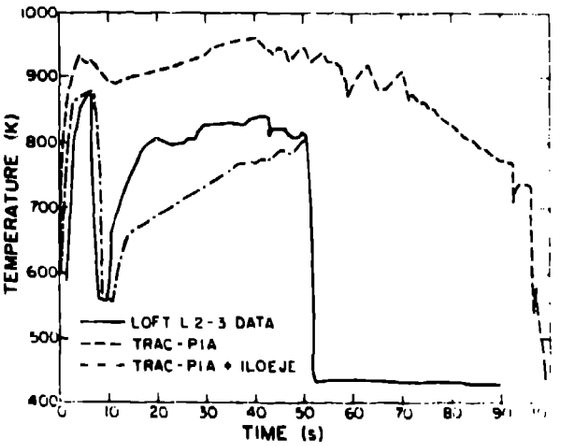

Fig. 28. TRAC pretest prediction of cladding temperature at core mid-plane for LOFT Test L2-3.

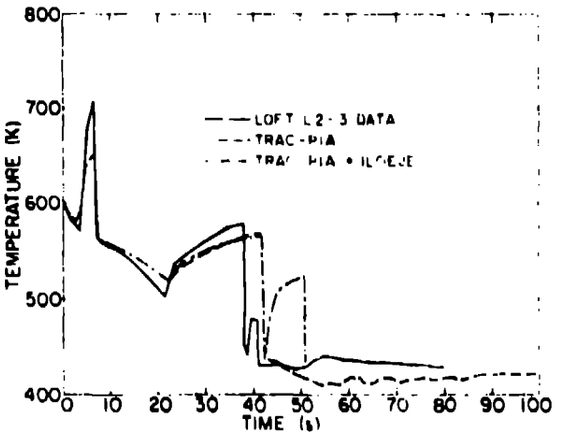

Fig. 29. TRAC pretest predictions of cladding temperature at outer core periphery for LOFT Test L2-3

with the data. In the higher power region near the center of the core, however, standard TRAC-P1A did not predict the early rewet, while the version with the Iloeje correlation did (see Fig. 28). These results again indicate that an improved film boiling correlation is necessary to calculate the rewet phenomena in LOFT. To decide on an appropriate correlation to be implemented in future release versions of TRAC, additional data from other facilities are currently being examined.

Difficulties in accurately predicting the dryout behavior in parts of the core were also observed. These appear to be related to the underprediction of the broken cold-leg flow during the first 5 s of the transient. Underprediction of the cold-leg break flow was mainly because vapor generation model in TRAC-P1A does not account for the effect of delayed nucleation. This problem was not evident in the broken loop hot leg because of the higher flow resistance and temperature. In general, the calculated behavior in the intact loop was qualitatively good.

Experience to date in predicting LOFT experiments has been encouraging. In particular, TRAC has done a good job of predicting the overall thermal-hydraulic behavior of the large-break LOCA tests. Areas where specific models needed to be improved have also been identified, however. For example, the tendency of TRAC-P1A to underpredict subcooled break flows, as mentioned above, was also observed in subsequent small-break test analyses. This has led to modeling improvements that will be incorporated into future code versions.

6. CONCLUSIONS

The material presented in this chapter illustrates that substantial progress has been made in meeting the need for reliable and efficient LWR safety analysis codes. The recent best-estimate codes provide increased predictive reliability through much more comprehensive modeling of important thermal-hydraulic phenomena and much more extensive and methodical assessment against experimental data. In addition, the replacement of user-controlled options and tuning dials with more fundamental modeling is enhancing the predictive credibility of these new codes.

As indicated earlier, much of the code development and assessment effort to date has been mainly directed toward the large-break LOCA. The blowdown and refill phases of these accidents can be well characterized with the available system codes, and steady progress is being made in modeling the reflood phase. Perhaps the most difficult issue remaining with regard to large-break LOCAs is establishing the ability of the codes to extrapolate to full-size PWR behavior.

Although much of the code development to date is also applicable to small break LOCAs and other postulated transients, some new modeling features are required. In addition, the codes must be very fast running to allow analysis of very long transients. These features are currently being emphasized in the development of RELAP5 and the fast running versions of the TRAC code. Considerable assessment remains to be done in this area.

The authors believe that the accurate and economical performance already achieved will be significantly improved. These codes can be used to examine a broad range of postulated accident conditions to assist in implementing improved designs and procedures for accident prevention and investigation. Additionally, codes with faster than real time running capability could potentially be used in on-line accident diagnostic systems that could allow operators to respond more effectively to off-normal conditions.

Finally, code development will continue to meet increasing needs for improved plant integrity and reliability, and assurance of safety system performance. These needs in the nuclear area are stimulated by our country's need for a stable, economical, and safe supply of energy. For the analyst and experimentalist in nuclear safety, these increasing needs mean greater demands and responsibilities for measurability in design and safety assessment techniques and rigor in their application.

REFERENCES

1. M. Ishii, Thermo-Fluid Dynamic Theory of Two-Phase Flow, Collection de la Direction des Etudes et Recherches d'Electricite de France, 22, xxix, p 248 (1975).

2. D. Gidaspow (Chairman), "Modeling of Two-Phase Flow," Proceedings of Round Table Discussion RT-1-2 at the Fifth International Heat Transfer Conference, Tokyo, Japan, Sepetember 3-7, 1974, also in Heat Trans., 3, 1974.

3. P. S. Anderson, P. Astrup, L. Eget, O. Kathmann, "Numerical Experience With the Two-Fluid Model, RISQUE," Proceedings of NAS Water Reactor Safety Meeting, July 31 - August 4, 1977.

4. R. Jackson, "The Present Status of Fluid Mechanical Theories of Fluidization," Chemical Engineering Progress Symposium Series, Number 105, Vol. 66, 1970.

5. J. D. Ramshaw and J. A. Trapp, "Characteristics, Stability and Short-Wave Length Phenomena in Two-Phase Flow Equation Systems," Aerojet Nuclear Company Report, ANCR-1272 (1976).

6. F. H. Harlow and R. Amsden, "Flow of Interpenetrating Material Phases," Journal of Computational Physics, 18 (1975) pp 440-464.

7. V. H. Ransom, et al., "RELAP5 Code Development," CDAP-TR-057 (VOL. I) (May 1979).

8. "TRAC-P1A - An Advanced Best-Estimate Computer Program for PWR LOCA Analysis," NUREG/CR-0665 (May 1979)

9. Emergency Core Cooling, Report of Advisory Task Force on Power Reactor Emergency Cooling, USAEC, W. K. Ergen, Chairman (1967).

10. "Acceptance Criteria for Emergency Core Cooling Systems for Light-Water Cooled Nuclear Power Reactors Pursuant to the AEC's Notice of Rule-Making Hearing 50-1," November 26, 1971, Concluded August 25, 1972, Concluding Statement of Position of the Regulatory Staff, Docket No. RM-50-1 (April 16, 1973).

11. "Water Reactor Safety Research Program, A Description of Current and Planned Research," NUREG-0006 (February 1979).

12. S. G. Margolis, J. A. Redfield, "FLASH: A Program for Digital Simulation of the Loss-of-Coolant Accident," WAPD-TM-534 (May 1966).

13. J. A. Redfield, J. H. Murphy, V. C. Davis, "FLASH-2: A FORTRAN/IV Program for the Digital Simulation of a Multinode Reactor Plant During Loss-of-Coolant," WAPD-TM-666 (April 1967).

14. F. V. Moore, L. C. Richardson, J. W. Sielinsky, "RELAPSE-1 - A Digital Program for Reactor Blowdown and Power Excursion Analysis," PTR-803 (September 1966).

15. F. V. Moore, W. H. Rettig, "RELAP2 -- A Digital Program for Reactor Blowdown and Power Excursion Analysis," IDO-17263 (March 1968).

16. W. H. Rettig, et al., "RELAP3 -- A Computer Program for Reactor Blowdown Analysis," IN-1321 (June 1970).

17. K. R. Katsma, G. L. Singer, T. R. Charlton, et al., RELAP4/MOD5 - A Computer Program for Transient Thermal-Hydraulic Analysis of Nuclear Reactors and Related Systems, User's Manual, Volumes I-III, ANCR-NUREG-1335. Volume I - RELAP4/MOD5 Descriptions, Volume II - Program Implementation, Volume III - Checkout Applications (September 1976).

18. S. R. Fisher, et al., "RELAP4-MOD6 - A Computer Program for Transient Thermal-Hydraulic Analysis of Nuclear Reactors and Related Systems," CDAP-TR-003 (January 1978).

19. S. R. Behling, "RELAP4/MOD7 - A Best-Estimate Computer Program to Calculate Thermal and Hydraulic Phenomena in a Nuclear Reactor of Related Systems," to be published.

20. L. J. Ybarrondo, C. W. Solbrig, H. S. Isbin, "The 'Calculated' Loss-of-Coolant Accident: A Review," AIChE Monograph Series, No. 7, (1972).

21. C. W. Solbrig, L. J. Ybarrondo, and R. J. Wagner, "Idaho Nuclear Code Automation: A Standardized and Modularized Code Structure," Proceedings of Conference on New Developments in Reactor Mathematics and Applications, CONF-710302, (Vol. 1) (March 29-31, 1971).

22. J. F. Wilson, R. J. Grenda, and J. F. Patterson, "The Velocity of Rising Steam in a Bubbling Two-Phase Mixture," Transactions of the American Nuclear Society (May 1962).

23. "Evaluation of LOCA Hydrodynamics," Regulatory Staff Technical Review, USAEC (November 1974).

24. R. J. Wagner, "HEAT 1--A One-Dimensional Time-Dependent or Steady-State Heat Conduction Code for the IBM-650," IDO-16867 (April 1963).

25. R. J. Wagner, "IREKIN - Program for the Numerical Solution of the Reactor Kinetics Equations," IDO-17114 (January 1966).

26. J. A. Dearien, L. J. Siefken, and M. P. Bohn, "FRAP-T3 - A Computer Code for the Transient Analysis of Oxide Fuel Rods," TFBP-TR-194 (August 1977).

27. T. A. Porsching, J. H. Murphy, J. A. Redfield, and V. C. Davis, "Flash-4 a Fully Implicit FORTRAN IV Program for the Digital Simulation of Transients in a Reactor Plant," WAPD-TM-840 (March 1969).

28. "Assessment of the RELAP4/MOD6 Thermal-Hydraulic Transient Code for PWR Experimental Applications - Addendum - Analysis Completed and Reported in FY 1979," EG G-CAAP-5022 (February 1980).

29. M. L. Patton, "Semiscale Mod-3 Test Program and System Descriptions," TREE-NUREG-1212 (July 1978).

30. V. Esparza, K. E. Sacket, and K. Stanger, "Experiment Data Report for Semiscale MOD-3 Integral Blowdown and Reflood Heat Transfer Test S-07-6 (Baseline Test Series)," NUREG/CR-0467, TREE-1226, (January 1979).

31. J. A. Trapp and V. H. Ransom, "RELAP5 Hydrodynamic Model: Program Summary - Field Equations," SRD-126-76, EG G Report (June 1976).

32. V. H. Ransom and J. A. Trapp, "RELAP5 Hydrodynamic Model: Progress Summary PILOT Code," PG-R-76-013, EG G Report (December 1976).

33. V. H. Ransom, et al., "RELAP5 Code Development and Results," Presented at the Fifth Water Reactor Safety Research Information Meeting (November 7-11, 1977).

34. V. H. Ransom, and J. A. Trapp, "RELAP5 Progress Summary, PILOT Code Hydrodynamic Model and Numerical Scheme," Idaho National Engineering Laboratory report No. CD-AP-TR-005 (January 1978).

35. O. C. Jones, Jr. and P. Saha, "Volumetric Vapor Generation in Nonequilibrium, Two-Phase Flows," Notes prepared for Advanced Code Review Group Meeting, Water Reactor Safety Research Division, U.S. Nuclear Regulatory Commission, Washington, D.C. 20555, (June 2, 1977).

36. G. Houdayer, et al., "Modeling of Two-Phase Flow with Thermal and Mechanical Nonequilibrium," paper presented at the Fifth Water Reactor Safety Research Information Meeting, Washington, D.C., (November 7-11, 1977).

37. A. W. Bennett, et al., "Flow Visualization Study of Boiling Water at High Pressure," AERE-R 4874 (1965).

38. R. T. Lahey, Jr., "RPI Two-Phase Flow Modeling Program," presented at Fifth Water Reactor Safety Research Information Meeting, (November 7-11, 1977).

39. N. Zuber, "On the Dispersed Two-Phase Flow in the Laminar Flow Region," Chemical Engineering Science, Vol. 19, (1964) pp 897-917.

40. K. T. Claxton, J. G. Collier, and A. J. Ward, "H.T.F.S. Correlation for Two-Phase Pressure Drop and Void Friction in Tubes," AERE-R7162 (1972).

41. V. H. Ransom and J. A. Trapp, "RELAP5 Progress Summary Analytic Choking Criterion for Two-Phase Flow," EG G Report, CDAP-TR-013 (1978).

42. V. H. Ransom and J. A. Trapp, "The RELAP5 Choked Flow Model and Application to a Large Scale Flow Test," presented at ASME Heat Transfer Division, Nuclear Reactor Thermal-Hydraulic 1980 Topical Meeting, Saratoga, New York.

43. J. A. Trapp and V. H. Ransom, "RELAP5 Hydrodynamic Model Progress Summary Abrupt Area Changes and Parallel Branching," PG-R-77-92, EG G Report (November 1977).

44. J. K. Vennard, Elementary Fluid Mechanics 4th Edition, John Wiley and Sons, 1965.

45. J. G. Collier, "Advanced Study Institute on Two-Phase Flows and Heat Transfer, ASI Proceedings, Istanbul, Turkey (August 1976).

46. K. F. Carlson, V. H. Ransom, and R. J. Wagner, "The Application of RELAP5 to a PIPE Blowdown Experiment," presented at ASME Heat Transfer Division, Nuclear Reactor Thermal-Hydraulic 1980 Topical Meeting, Saratoga, New York.

47. H. H. Kuo, V. H. Ransom, and D. M. Snider, "Calculated Thermal Hydraulic Response for Semiscale Mod-3 Test S-07-6 Using RELAP5--A New LWR System Analysis Code," Presented at the ASME Heat Transfer Division Nuclear Reactor Thermal-Hydraulic 1980 Topical Meeting, Saratoga, New York.

48. E. J. Kee, et al., "Best-Estimate Prediction for LOFT Nuclear Experiment L3-2," EG G-LOFF-5089 (February 1980).

49. "TRAC-P1: An Advanced Best-Estimate Computer Program for PWR LOCA Analysis. Vol. I: Methods, Models, User Information, and Programming Details," Los Alamos Scientific Laboratory report LA-7279-MS, Vol. I (NUREG/CR-0063) (June 1978).

50. J. C. Vigil and K. A. Williams (Compilers), "TRAC-P1A Developmental Assessment Calculations," Los Alamos Scientific Laboratory report LA-8056-MS (NUREG/CR-1059) (October 1979).

51. F. H. Harlow and A. R. Amsden, "A Numerical Fluid Dynamics Calculation Method for All Flow Speeds," J. Comp. Physics 8, 197 (1971).

52. F. H. Harlow and A. R. Amsden, "KACHINA: An Eulerian Computer Program for Multifield Fluid Flows," Los Alamos Scientific Laboratory report LA-5680 (1975).

53. D. R. Liles and W. H. Reed, "A Semi-Implicit Method for Two-Phase Fluid Dynamics," accepted for publication in J. of Comp. Physics.

54. J. H. Mahaffy and D. R. Liles, "Application of Implicit Numerical Methods to Problems in Two-Phase Flow," Los Alamos Scientific Laboratory report LA-7770-MS (1979).

55. C. J. Crowley, J. A. Block, and C. N. Cary, "Downcomer Effects in a 1/15-Scale PWR Geometry - Experimental Data Report," Creare, Inc. report NUREG-0281 (May 1977).

56. L. J. Ball, D. J. Hanson, K. A. Dietz, and D. J. Olson, "Semiscale MOD-1 Test S-02-8 (Blowdown Heat Transfer Test)," Aerojet Nuclear Company report ANCR-NUREG-1238 (August 1976).

57. D. L. Reeder, "LOFT System and Test Description (5.5-ft Nuclear Core 1 LOCES)," EG G Idaho, Inc. report TREE-1208 (NUREG/CR-0247) (July 1978).

58. P. G. Prassinos, B. M. Galusha, and D. B. Engleman, "Experiment Data Report for LOFT Power Ascension Experiment L2-3," Idaho National Engineering Laboratory report TREE-1326 (NUREG/CR-0792) (July 1979).

59. O. C. Iloeje, D. N. Plummer, W. M. Rohsenow, and P. Griffith, "An Investigation of the Collapse and Surface Rewet in Film Boiling in Forced Vertical Flow," J. of Heat Transfer, pp 166-172 (May 1975).

APPENDIX A - REVIEW OF SOME NUMERICAL TECHNIQUES USED IN LWR SAFETY CODES

A.1 INTRODUCTION

Any reasonable set of equations that could be used to describe the thermal hydraulics of a nuclear reactor under accident conditions would be far too complex to allow analytic solutions. The increasingly sophisticated digital computers that are available for scientific purposes do allow numerical simulations of the fluid mechanics and heat transfer, however. Two fundamental difficulties with any numerical procedure are: (a) approximations must be made that may not always preserve the exact character of the original equations and (b) insights into the solutions (such as unstable regions, peak variable values, etc.) are not attained as readily as with analytical solutions. Despite these difficulties, numerical modeling can provide information on the response of the whole system that cannot otherwise be obtained. This Appendix covers some of the aspects of hydrodynamic modeling of large reactor systems using finite difference schemes.

A.2 FINITE DIFFERENCE EQUATIONS

Consider the following set of hydrodynamics equations

$$\frac{\partial \rho}{\partial t} + \frac{\partial}{\partial x} \rho V = 0 \tag{A-1}$$

$$\rho \frac{\partial V}{\partial t} + \rho V \frac{\partial V}{\partial x} + \frac{\partial P}{\partial x} = 0 \tag{A-2}$$

$$\rho = \rho (P) \quad . \tag{A-3}$$

Here, ρ is the density, V the velocity, and P the pressure.

We wish to approximate the partial differential equations in such a way that a digital computer can integrate the equations in space and time with a consistent technique (i.e., one which in the limit as $\Delta t \to 0$ and $\Delta x \to 0$ returns a solution of the original differential equations).

Although there are a vast number of procedures that could be used, all of the current major reactor system codes (TRAC, RELAP5, and COBRA TF) employ the same basic difference scheme and solution technique. This particular scheme is relatively easy to code, is stable for moderate time-step sizes, and is robust and reliable.

The spacial differencing uses a staggered mesh[A-1]--staggered because the momentum equations are written over volumes half a mesh cell up or downstream from the volumes over which the scalar field equations are provided. The heavy lines in the following figure indicate a typical 1-D computational mesh, while the dotted lines show where the momentum equations will be written

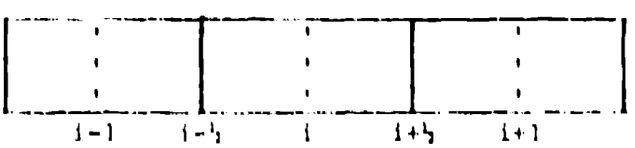

The subscript i indicates a mesh cell center. All the thermodynamic variables, i.e., ρ and p, are located at the center of the scalar cells, while the velocities are located at the center of the momemtum cells (scalar cell edges).

Reference A-2 by Liles and Reed provides a more complete description of the solution procedure that is now delineated. A finite difference approximation to Eq. (A-1) becomes:

$$\frac{\rho_i^{n+1} - \rho_i^n}{\Delta t} = \frac{\left(\rho^n v^{n+1}\right)_{i-\frac{1}{2}} - \left(\rho^n v^{n+1}\right)_{i+\frac{1}{2}}}{\Delta x} \quad , \tag{A-4}$$

where the superscript n implies the old time quantities and n+1 implies the new time quantities. The momentum equation, Eq. (A-2), becomes

$$\frac{v_{i+\frac{1}{2}}^{n+1} - v_{i+\frac{1}{2}}^n}{\Delta t} = -v_{i+\frac{1}{2}}^n \left(\frac{v_{i+1}^n - v_i^n}{\Delta x}\right) - \frac{1}{\rho_{i+\frac{1}{2}}} \left(\frac{p_{i+1}^{n+1} - p_i^{n+1}}{\Delta x}\right) \quad . \tag{A-5}$$

The time levels for the convective terms are chosen to allow the wave speed Courant limit $\frac{(V+c)\Delta t}{\Delta x}$ to be violated (see Ref. A-3), but not the material Courant limit, $\frac{V\Delta t}{\Delta x} < 1$. In these expressions C is the speed of sound and V is the material velocity. It should be noted that Eq. (A-5) can be rewritten as:

$$v_{i+\frac{1}{2}}^{n+1} = \tilde{v}_{i+\frac{1}{2}} - \frac{\Delta t}{\rho_{i+\frac{1}{2}} \Delta x} \left(\delta p_{i+1} - \delta p_i\right) \quad , \tag{A-6}$$

where $$\tilde{v}_{i+\frac{1}{2}} = v_{i+\frac{1}{2}}^n - v_{i+\frac{1}{2}} \frac{\Delta t}{\Delta x} \left(v_{i+1}^n - v_i^n\right) - \frac{\Delta t}{\rho_{i+\frac{1}{2}}} \left(\frac{p_{i+1}^n - p_i^n}{\Delta x}\right) \quad , \tag{A-7}$$

and $$\delta p_i = p_i^{n+1} - p_i^n \quad , \tag{A-8}$$

which is the pressure change during the time step.

We shall next linearize the equation-of-state

$$d\rho = \frac{\partial \rho}{\partial p} dp \tag{A-9}$$

and write a first order Taylor series expansion for ρ_i^{n+1}, i.e.,

$$\rho_i^{n+1} = \rho_i^n + \left(\frac{\partial \rho_i}{\partial p}\right)^n dp_i \quad . \tag{A-10}$$

Combining (A-4), (A-6), (A-9), and (A-10), we obtain (one more momentum equation must be written for $v_{i-\frac{1}{2}}^{n+1}$)

$$\left(\frac{\partial\rho}{\partial P}\right)_i^n \delta P_i = \frac{\delta t}{\delta x}\left[\rho_{i-\frac{1}{2}}^n\left(\tilde{V}_{i-\frac{1}{2}} + \frac{\Delta t}{\Delta x}\frac{1}{\rho_{i-\frac{1}{2}}^n}\left(\delta P_{i-1} - \delta P_i\right)\right)\right.$$

$$\left. - \rho_{i+\frac{1}{2}}^n\left(\tilde{V}_{i+\frac{1}{2}} + \frac{\Delta t}{\Delta x}\frac{1}{\rho_{i+\frac{1}{2}}^n}\left(\delta P_i - \delta P_{i+1}\right)\right)\right] \quad . \tag{A-11}$$

It should be noted that in order to complete the finite difference scheme, variable values are required at locations where they are not defined. Auxiliary equations are needed to obtain closure. To obtain stability, donor cell averages are used.

$$\rho_{i+\frac{1}{2}} = \rho_i \text{ , if } V_{i+\frac{1}{2}} \geq 0$$

$$\rho_{i+\frac{1}{2}} = \rho_{i+1} \text{ , if } V_{i+\frac{1}{2}} < 0 \quad . \tag{A-12}$$

It should be noted that pressures in the momentum equation cannot be donor celled. If they were, waves could not always propagate in all directions and stagnation regions could be uncoupled from the remainder of the flow field. One of the great virtues of the staggered difference scheme is that close coupling of the pressure gradient term occurs naturally with the velocity and results in diagonally dominant matrices (if $\frac{V\Delta t}{\Delta x} < 1$).

A.3 SOLUTION STRATEGY

This provides us with a tridiagonal matrix in pressure to solve. Direct elimination or a Gauss-Seidel iteration can be used. The total calculational sequence occurs as follows: (a) a first pass over the mesh for Eq. (A-7) provides "trial" new time velocities, (b) Eq. (A-11) is solved for pressure with all the old-time quantities known either from initialization or the previous timestep, (c) the thermodynamic equation-of-state (Eq. (A-3)) is solved for the new densities. This finishes one timestep.

A.4 1-D DRIFT-FLUX EQUATIONS IN TRAC

This same technique can be used for the more complicated two-phase flow equations in reactor safety codes. A minimum model that describes adequately both thermal and velocity nonequilibrium is the five equation drift-flux model. This approach is used in the 1-D components in TRAC. The following text develops these equations and describes how they are solved.

Field Equations. The differential field equations[A-4] for the two-phase, five-equation drift-flux model are given below. The subscripts g and f refer to the gas and liquid phase, and m denotes mixture quantities. α is the volume fraction of the vapor.

Mixture Mass Equation

$$\frac{\partial}{\partial t} \rho_m + \frac{\partial}{\partial x} (\rho_m V_m) = 0 \qquad \text{(A-13)}$$

Vapor Mass Equation

$$\frac{\partial}{\partial t} (\alpha\rho_g) + \frac{\partial}{\partial x} (\alpha\rho_g V_m) + \frac{\partial}{\partial x} \left[\frac{\alpha\rho_g (1-\alpha)\ \rho_\ell V_r}{\rho_m}\right] = \Gamma \qquad \text{(A-14)}$$

Mixture Equation of Motion

$$\frac{\partial}{\partial t} V_m + V_m \frac{\partial}{\partial x} V_m + \frac{1}{\rho_m} \frac{\partial}{\partial x} \left[\frac{\alpha\rho_g (1-\alpha)\ \rho_\ell V_r^2}{\rho_m}\right] = -\frac{1}{\rho_m} \frac{\partial p}{\partial x} - K V_m |V_m| + g \qquad \text{(A-15)}$$

Vapor Thermal Energy Equation

$$\frac{\partial}{\partial t} (\alpha\rho_g e_g) + \frac{\partial}{\partial x} (\alpha\rho_g V_m e_g) + \frac{\partial}{\partial x} \left[\frac{\alpha\rho_g (1-\alpha)\ \rho_\ell V_r e_g}{\rho_m}\right] + p \frac{\partial}{\partial x} (\alpha V_m)$$

$$+ p \frac{\partial}{\partial x} \left[\frac{\alpha(1-\alpha)\ \rho_\ell}{\rho_m} V_r\right] = q_{wg} + q_{ig} - p \frac{\partial \alpha}{\partial t} + \Gamma h_{sg} \qquad \text{(A-16)}$$

Mixture Thermal Energy Equation

$$\frac{\partial}{\partial t} (\rho_m e_m) + \frac{\partial}{\partial x} (\rho_m e_m V_m) + \frac{\partial}{\partial x} \left[\frac{(1-\alpha)\ \rho_\ell \alpha\rho_g (e_g - e_\ell)}{\rho_m} V_r\right] + p \frac{\partial V_m}{\partial x}$$

$$+ p \frac{\partial}{\partial x} \left[\frac{\alpha(1-\alpha)(\rho_\ell - \rho_g)}{\rho_m} V_r\right] = q_{wf} + q_{wg} \qquad \text{(A-17)}$$

where

$$\rho_m = \alpha\rho_g + (1-\alpha)\rho_\ell \qquad \text{(A-18)}$$

$$V_m = \frac{\alpha\rho_g V_g + (1-\alpha)\,\rho_\ell\, V_\ell}{\rho_m} \quad , \tag{A-19}$$

and

$$V_r = V_g - V_\ell \quad . \tag{A-20}$$

The expression for e_m is the same as Eq. (A-19) with V replaced by e. In addition to the thermodynamic relations that are required for closure, specifications for the relative velocity (V_r), the interfacial heat transfer (q_{ig}), the phase change rate (Γ), the wall shear coefficient (K), and the wall heat transfers (q_{wg} and $q_{w\ell}$) are required. The correlations used for these quantities will not be discussed. Gamma can be evaluated from a simple thermal energy jump relation

$$\Gamma = \frac{-q_{ig} - q_{i\ell}}{h_{sg} - h_{s\ell}} \quad , \tag{A-21}$$

where

$$q_{ig} = h_{ig}A_i\,(T_s - T_g)/\text{vol} \tag{A-22}$$

and

$$q_{i\ell} = h_{i\ell}A_i\,(T_s - T_\ell)/\text{vol} \tag{A-23}$$

The quantities h_{ig}, $h_{i\ell}$, and A_i are evaluated using a complicated estimate of the flow regime interfacial heat transfers.

Wall heat transfer terms assume the form:

$$q_{wg} = h_{wg}A_{wg}(T_w - T_g)/\text{vol} \tag{A-24}$$

and

$$q_{w\ell} = h_{w\ell}A_{w\ell}(T_w - T_\ell)/\text{vol} \tag{A-25}$$

Finite Difference Equations. The one-dimensional flow equations in TRAC have been written in two separate finite difference forms. The first form of the difference equations is semi-implicit and has a time step size stability limit of the form

$$\Delta t < \left|\frac{\Delta x}{V}\right| \quad ,$$

where Δx is the mesh spacing and V the fluid velocity. In blowdown problems, this time step is usually prohibitively small due to the high velocities near

the break. To alleviate this problem, a set of unconditionally stable, fully-implicit difference equations was written for use in pipes where the fluid velocities are expected to be high. Only the first semi-implicit set will be considered.

The equations are solved for one-dimensional pipes using the staggered difference scheme on the Eulerian mesh. State variables such as pressure, internal energy, and void fraction are obtained at the center of the mesh cells, which have length Δx_j, and the mean and relative velocities are obtained at the cell boundaries. Because of this staggered difference scheme, it is necessary to form spatial averages of various quantities to obtain the finite difference form of the divergence operators. To produce stability in the partially implicit method, a donor-cell average is used of the form,

$$\langle YV \rangle_{j+\frac{1}{2}} = Y_j V_{j+\frac{1}{2}} \qquad \text{for } V_{j+\frac{1}{2}} \geq 0$$

$$= Y_{j+1} V_{j+\frac{1}{2}} \qquad \text{for } V_{j+\frac{1}{2}} < 0 \ , \tag{A-26}$$

where Y is any state variable or combination of state variables. An integer subscript indicates that a quantity is evaluated at mesh cell center and a half integer denotes that it is obtained at a cell boundary. With this notation, the finite difference divergence operator is

$$\nabla_j (YV) = (A_{j+\frac{1}{2}} \langle YV \rangle_{j+\frac{1}{2}} - A_{j-\frac{1}{2}} \langle YV \rangle_{j-\frac{1}{2}})/\mathrm{vol}_j \ , \tag{A-27}$$

where A is the cross-section area, and vol_j is the volume of the j^{th} cell. Slight variations of these donor-cell terms appear in the velocity equation of motion. Donor-cell averages are of the form

$$\langle YV_r^2 \rangle_j = Y_j V_{r,j-\frac{1}{2}}^2 \qquad \text{for } V_{r,j-\frac{1}{2}} \geq 0$$

$$= Y_j V_{r,j+\frac{1}{2}}^2 \qquad \text{for } V_{r,j+\frac{1}{2}} < 0 \tag{A-28}$$

and the donor-cell of the term $V_m \nabla V_m$ is

$$V_{m,j+\frac{1}{2}} \nabla_{j+\frac{1}{2}} V_m = V_{m,j+\frac{1}{2}} (V_{m,j+\frac{1}{2}} - V_{m,j-\frac{1}{2}})/\Delta x_j \qquad \text{for } V_{m,j+\frac{1}{2}} \geq 0$$

$$= V_{m,j+\frac{1}{2}} (V_{m,j+\frac{3}{2}} - V_{m,j+\frac{1}{2}})/\Delta x_{j+1} \qquad \text{for } V_{m,j+\frac{1}{2}} < 0 \ . \tag{A-29}$$

Given the preceding notation, the finite difference equations for the partially implicit method are:

Mixture Mass Equation

$$(\rho_m^{n+1} - \rho_m^n)_j/\Delta t + \nabla_j(\rho_m^n V_m^{n+1}) = 0 \quad , \tag{A-30}$$

Vapor Mass Equation

$$(\alpha^{n+1}\rho_g^{n+1} - \alpha^n\rho_g^n)_j/\Delta t + \nabla_j(\alpha^n\rho_g^n V_m^{n+1}) + \nabla_j(\rho_f^n V_r^n) = \Gamma \quad , \tag{A-31}$$

Mixture Energy Equation

$$(\rho_m^{n+1}e_m^{n+1} - \rho_m^n e_m^n)_j/\Delta t + \nabla_j(\rho_m^n e_m^n V_m^{n+1}) + \nabla_j\left[\rho_f^n(e_g^n - e_\ell^n)V_r^n\right]$$
$$= -p_j^{n+1}\nabla_j\left\{V_m^{n+1} + \left[\rho_f^n\left(\frac{1}{\rho_g^n} - \frac{1}{\rho_\ell^n}\right)V_r^n\right]\right\} + q_{j,wg} + q_{j,w\ell} \quad , \tag{A-32}$$

Vapor Energy Equation

$$\left[(\alpha\rho_g e_g)^{n+1} - (\alpha\rho_g e_g)^n\right]_j/\Delta t + \nabla_j(\alpha^n\rho_g^n e_g^n V_m^{n+1}) + \nabla_j(\rho_f^n e_g^n V_r^n) + p^{n+1}\nabla_j(\alpha^n V_m^{n+1})$$
$$+ p^n\nabla_j(\rho_f^n V_r^n/\rho_g^n) = -p_j^{n+1}(\alpha_j^{n+1} - \alpha_j^n)/\Delta t + (q_{wg} + q_{i_g} + \Gamma h_{sg}^{n+1})_j \quad , \tag{A-33}$$

Mixture Equation of Motion

$$(V_m^{n+1} - V_m^n)_{j+\frac{1}{2}}/\Delta t + V_{m,j+\frac{1}{2}}^n \nabla_{j+\frac{1}{2}} V_m^n$$
$$= -\left\{(p_{j+1}^{n+1} - p_j^{n+1})/\Delta x_{j+\frac{1}{2}} + \nabla_{j+\frac{1}{2}}(\rho_f V_r^2)^n\right\}/\bar{\rho}_{m,j+\frac{1}{2}}^n + g^n - K^n V_m^{n+1}\left|V_m^n\right| \quad , \tag{A-34}$$

where

$$\overline{\Delta x}_{j+\frac{1}{2}} = (\Delta x_j + \Delta x_{j+1})/2 \quad , \tag{A-35}$$

$$\rho_f^n = \frac{\alpha^n(1-\alpha^n)\ \rho_g^n\ \rho_\ell^n}{\rho_m^n} \quad , \tag{A-36}$$

and

$$\begin{aligned} \bar{\rho}^n_{m,j+\frac{1}{2}} &= \rho^n_{m,j} && \text{for } V_{j+\frac{1}{2}} \geq 0 \\ &= \rho^n_{m,j+1} && \text{for } V_{j+\frac{1}{2}} < 0 \quad . \end{aligned} \tag{A-37}$$

If the appropriate caloric and equations-of-state are inserted and a first-order Taylor series is used to evaluate the new time state quantities, we obtain block tridiagonal matrices in the variables α, P, T_L, T_V. These can then be solved and passes made through the thermodynamics to obtain new densities and energies for both phases. This basic numerical procedure extends to the two fluid model and may be also used in multiple spacial dimensions (although the resulting arrays are no longer tridiagonal).

This Appendix will not address a wide range of numerical problems such as numerical diffusion, numerical viscoscity, and formal trunciation accuracy. Reference A-3 contains discussions of some of these other important points.

A.5 REFERENCES

A-1. F. H. Harlow and A. R. Amsden, J. of Comp. Physics 18, p 40 (1975).

A-2. D. R. Liles and W. H. Reed, J. of Comp. Physics 26, p 390 (1973).

A-3. P. J. Roache, Computational Fluid Dynamics, Hermosa Publishers, Albuquerque, New Mexico (1976).

A-4. M. Ishii, "Thermo-Fluid Dynamic Theory of Two-Phase Flow," Eyrolles, Paris (1975).